Journal of Engineering Materials and Technology (JEMT), 2017

Atomistic fault energetics and critical stress prediction for fcc and bcc twinning: Recent progress

Piyas Chowdhury, Huseyin Sehitoglu *

Department of Mechanical Science and Engineering, University of

Illinois at Urbana-Champaign, 1206 W. Green St., Urbana, IL 61801, USA

* Corresponding Author, e-mail address: huseyin@illinois.edu

Tel: +1 217 333 4112

Fax: +1 217 244 6534

Abstract

This article recounts recent advances on the atomistic modeling of twinning in bcc and fcc alloy. Specifically, we have reviewed: (i) the experimental evidence of twinning-dominated deformation in single- and multi-grain microstructures (ii) calculation of generalized planar fault energy landscapes, and (iii) the prediction of critical friction stresses to initiate twinning-governed plasticity (e.g. twin nucleation, twin-slip and twin-twin interactions). Possible avenues for further research are outlined.

Keywords

Twinning; stacking fault energy; metallic materials; electron microscopy; atomistic modeling

1. Introduction

Formation of various defects (e.g. slip, twin) and their interactions with interfaces constitute the microscopic deformation scenario [1]. At the atomic level, the stacking fault energy landscape (also known as the γ surface) is a crucial signature of a specific fault nucleation. It is suggested that the exact nature of the γ energy surface would dictate the initiation of a specific defect (i.e. slip or twinning) at the elasto-plastic juncture [2-5]. The exact magnitude of this important energetic parameter is a function of the extent of solid solution, solute segregation, and volumetric misfit among atoms of different chemical species. Recent

studies have noted interesting utilization of the γ surface in formulating critical resolved shear stresses for twinning in fcc and bcc alloys. The phenomenon of twinning is of paramount importance due to the associated enhanced toughening attributes as manifested in experiments [6-8].

Significant physical contribution to the micromechanism of deformation originates from the discrete lattice-scale governing principles [9, 10]. At continuum lengthscale, the current description of deformation mechanics is of phenomenological nature [11-13]. At the smallest lengthscale, however, the material building blocks consist of discrete atoms. The laws of inter-atomic interactions are drastically different from the continuum laws suitable for describing bulk materials behaviors. The atomic-level deformation scenario is governed by the Schrodinger's equation [14] addressing electronic structure while the laboratory-scale deformation are best captured by empirical elasto-plastic laws. Despite the apparent dissimilarity among these largely spanned physical lengthscales, subtle effects at the atomic-scale would reverberate across the length scales, eventually contributing towards the observed continuum-scale mechanical behaviors [2]. For instance, the fault energetics is subjected to addition of certain solute types, which would essentially modify the energies from the base metal levels [3-5]. This in turn would alter what defect mechanism would be predominant (such as slip versus twinning) during the early plastic deformation periods. In particular, the defect formation propensity at the elasto-plastic juncture is crucial, in that the subsequent evolution of plasticity would be largely controlled by the predominant defects. The outcomes of mesoscopic plastic events would eventually decide the exact nature of the macroscale constitutive behaviors. Thus, establishing the energy landscape is an important step in the physical understanding of the alloy plastic behavior. The physical mechanisms of deformations (e.g. slip, twinning) can be qualitatively studied through atomic scale simulations. Moreover, the quantification of intrinsic defect generation can be elucidated from an atomistically-based methods [15, 16].

From a modeling perspective, it has long remained a challenging task to transition from atomic scales to meso- or to a higher lengthscale [17, 18]. Consideration of atomic phenomena in modeling is non-trivial, in that the propensity to seek the energetic ground state at the lattice scale dictates the exact nature of nucleated defects during plastic deformation (i.e. slip or twinning). Nonetheless, such theoretical efforts are compounded by the requirement of high computational capacity to simulate the mesoscale phenomena. Microscopically, there are the consideration of material interfaces being intercepted by other propagating defects (such as twin and/or slip) [19-21] to a gradually increasing degree. The specific nature of the interception

mechanism, and their relative predominance essentially plays a major role in the local deformation on a grain by grain basis. For example, dislocation transmission [22, 23], lock formation [24, 25], incorporation into boundaries [26, 27] and dislocation multiplication [28] at the interfaces constitute some of the most significant interactions that can physically occur. The energetic scenario of these physical mechanisms, if extracted accurately, can provide a sound basis for understanding their relative predilections. Depending on the boundary type, texture etc. certain reactions may be preferred. However, the γ surface can serve as a unique signature for a certain plastic mechanism in a pristine crystal setting. The two most widely used simulation methods to study the foregoing problems are *molecular dynamics (MD)* and *density functional theory (DFT)*. Interested readers are referred to the text books By Tadmor-Miller and Frenkel-Smit [14, 29], which narrate the particulars of these modeling methods.

To develop an in-depth understanding of such small length scale phenomena, today one needs a synergy of experimental study and computer simulations. For example, the changes in microstructure due to deformation are manifested as strain gradients, which can be detected with experimental techniques. The predominant defect types can then be studied with advanced digital image correlation (DIC), electron microscopy (TEM and SEM) and electron backscatter diffraction (EBSD). These experimental characterizations can form the basis of modeling. In the paper, we begin with examples on Co-Ni and Fe-Cr alloys On the modeling ground, we will extensively discuss the use of the γ energetics concepts to rationalize twinning phenomena. In that regard, it is important to note here that comprehensive reviews related to deformation twinning are duly recorded in the literature. For example, the survey by Christian [30] deals with experimental behaviors and phenomenological theories. More recently, review works by Beyerlein, Zhu and their co-workers [31, 32] describe the mechanisms of twinning in the nanocrystalline microstructure. In the current paper, we discuss only the mechanistic aspects related to the discrete lattice energetics. Overall, we envision that superior predictive capabilities useful for industrial-level applications would ultimately emerge through the sequential multiscale studies, which combine atomic-scale physics with mesoscale phenomenology (Figure 1).

The paper is organized as follows. In section 2, we briefly overview some latest experimental characterization results, which reveal twinning-mediated plasticity in representative alloys. Then, we summarily critique historically important models in section 3, and how these models motivated further refinement. Section 4 introduces the concept of the atomistic fault energetics and its significance in the metal plasticity. In section 5, we first overview historical models for predicting twinning stress, and then describe the latest stress-

prediction schemes utilizing fault energetics. The topic of annealing twins, their roles in slip transfer, extension of energetic models in mechanistically interpreting plastic flow and predicting critical stresses are discussed in section 6. In section 7, we outline potential avenues of further research, which are emerging alongside the current topics such as polycrystalline deformation, fracture mechanism, hcp deformation, phase transformation. We conclude in section 8 by commenting on the proper use of atomistics in further research and their potential usefulness in understanding larger lengthscale plastic deformation.

2. Brief discussion of experimental results

This section contains a brief overview of recent experimental findings on the deformation behavior of: (a) single crystals and polycrystals of bcc Fe-47.8%Cr (atomic), (b) single crystals of fcc Co-33%Ni alloys and (c) polycrystals of Ni-x%Co alloys of various Co contents (where, x = 1, 1.62, 2.9 and 5.6). The reason for selecting these case studies for discussion is that comprehensive atomistic modeling has also been undertaken on the same materials. Hereafter, we refer to the materials as Fe-Cr, Co-Ni and Ni-Co alloys respectively.

2.1 Deformation of Co-Ni single crystals and nano-twinned Ni-Co polycrystals

In Figure 2(a), the single-crystal Co-Ni alloys of fcc crystal structure is deformed in tension along $\langle 111 \rangle$ direction. The stress-strain response up to a resolved strain level of 1% is shown. Low-resolution DIC measurement conducted in-situ shows non-interacting parallel strain bands corresponding to $(1\bar{1}1)[121]$ twin system. This system experienced the maximum Schmid factor of 0.47. The EBSD scan indicates a crystal misorientation of 60^o between the strain band and the matrix material (i.e. suggestive of twinning). The TEM micrographs further confirm the presence of nano-scale deformation twins. Throughout the deformation range, additional parallel and non-interacting twins nucleate. These twins propagate and intercept slip sub-structure, resulting in the twin migration process. No twin-twin interaction is observed up to a resolved strain level of 1%. It should be noted that at higher strain the secondary systems are likely to activate, resulting in more complex strain band patterns.

Similar observations are made for the specimens compressed along $\langle 001 \rangle$ direction as in Figure 2(b). The (resolved) stress-strain curve along with the microstructure characterization (via DIC, EBSD and TEM) are presented. The single crystal under $\langle 001 \rangle$ compression deforms predominantly via twinning. In another case, post-deformation microstructures of $\langle 123 \rangle$ tension

and $\langle 111 \rangle$ compression case unveil a plastic mechanism dominated entirely by slip on the maximum Schmid factor system (not shown). In other words, either slip or twinning is triggered only when the maximum resolved shear stress for either system is reached.

Figure 2(c) presents the differences in the stress-strain responses for four compositions of Ni-Co alloys (with 1%, 1.62%, 2.9% and 5.52% Co contents) [33]. The microstructure of each alloy is characterized by a significant presence of annealing twins (unlike the Co-Ni cases, which experienced nucleation of twins during deformation). The deformed microstructure of the Ni-2.9%Co shows a buildup of slip around the twin boundaries as the TEM image shows. Despite very similar microstructure (in terms of twin and grain distributions), their plastic strengths, however, show a non-uniform trend with respect to Co content. The flow stress increases from 1%Co to 2.9%Co and then drops for the case of 5.52%Co. As we will discuss in subsequent sections, the physical origin of twinning-dominated plasticity in Co-Ni alloys, the composition effects in Ni-Co alloys etc. can be rationalized in the light of alloying-induced fault energy surfaces.

2.2 Deformation of Fe-Cr single crystals and polycrystals

As in Figure 3(a), during tension along $[0\bar{1}0]$ direction, the single crystal first undergoes slip nucleation on the $[\bar{1}1\bar{1}](121)$ system [34]. The critical resolved shear stress, τ_{CRSS}^{slip}, for the active slip system was determined to be 85 MPa. An abrupt load drop was noted marking the point where twin nucleation occurs. The critical resolved shear stress for twin nucleation τ_{CRSS}^{twin} was measured to be 177 MPa. By determining the possible systems with the maximum Schmid factors, the interacting strain bands (in SEM and DIC images) are identified as the twinning systems: $[11\bar{1}](12\bar{1})$ and $[11\bar{1}](\bar{1}21)$. The further confirmation of the strain bands of the $\langle 111 \rangle (121)$ type twins is obtained from the EBSD scan. Subsequent rise in the flow stress leads to the twin migration process (i.e. slip or another twin intercepting the previous twin).

Similarly, for the $[101]$ compression, the slip nucleation occurs at τ_{CRSS}^{slip} = 87 MPa and the twin nucleation at τ_{CRSS}^{twin} = 202 MPa as in Figure 6(b). Prior to the initiation of twinning, there exists a flow stress plateau, which is presumably caused by a significant build-up of the slip localization, a precursor to the twinning process. This inference is supported by the DIC observation that a greater distribution of localized strain is noted for $[101]$ compression. The

active slip systems were determined as $[1\bar{1}1](121)$ type (not shown). Following substantial amount of slip accumulation, twinning shear bands are found to have nucleated as the $[1\bar{1}1](121)$ and $[1\bar{1}1](1\bar{2}1)$ types.

The stress-strain response of the polycrystalline Fe-Cr alloys is presented in Figure 3(c) [35]. No flow stress drop occurs in this case. The DIC image demonstrates considerable degree of local straining in the form of non-interacting parallel bands (caused by slip) in individual grains. The strain bands are deflected at the grain boundaries. The suppression of twinning is presumably facilitated by the presence of grain boundaries. It is worth recalling that higher resolution images are typically required for resolving strains for polycrystalline microstructure. This is because the primary purpose is to determine how strain transfer occurs at the grain boundaries. To that end, a large area of interest spanning several grains were selected for DIC measurement, which in turn required very high resolution ex-situ measurement. On the other hand, the strain bands can be detected with more ease in single crystals with relatively small resolution. The DIC images for the Fe-Cr polycrystal in Fig 2(c) are performed ex-situ by digitally stitching 140 correlated images to accurately map the strain contours. Such precision was not employed for the case in Fig 2(a), where only one image (per load step) is analyzed to detect the presence of strain bands.

3. Brief overview of classical mechanistic models of twin nucleation

3.1 Pole mechanism (bcc)

Cottrell and Bilby [36] originally envisioned the formation of an embryonic mechanical twin in bcc lattice via the so-called pole mechanism. Figure 4 illustrates the mechanism leading to a three-layer twin nucleation. Triggered by applied loads, a perfect dislocation of the type $\frac{a}{2}[111]$ lying on the (112) plane dissociates into two dislocations: $\frac{a}{3}[112]$ and $\frac{a}{6}[11\bar{1}]$. The dislocation $\frac{a}{3}[112]$ is a sessile one of pure edge type, and acts as an anchor i.e. the so-called "pole" on the (112) plane. The partial dislocation $\frac{a}{6}[11\bar{1}]$ moves away from the pole i.e. bows out and creates a plane of stacking fault (gray portion) which is co-planar with the pole. Since the $\frac{a}{6}[11\bar{1}]$ dislocation is curved, it would have segments consisting of pure screw type. The

pure screw portion of the expanding loop cross-slips into another $\{112\}$-type plane i.e. $(\bar{1}21)$ or $(2\bar{1}1)$. The cross-glided partial sweeps around the pole, and thus creates a mono-layer stacking fault (red). This sweeping dislocation climbs into the adjacent parallel plane, and sweeps around the pole to create the second layer of stacking fault (blue). In the process, the twining partial bypasses the previous layer by a separation distance of $\frac{a}{\sqrt{6}}$. Under continued applied loads, the twinning dislocation spiral upwards, and in the process adds more layers to the initial one.

The expression for the critical twin nucleation stress based on the pole mechanism is: $\tau_{CRSS}^{twin} = \frac{\gamma_{us}}{b}$, where the γ_{us} is the unstable stacking fault energy (maximum energy in generalized stacking fault energy curve). For example, using γ_{us} magnitude of 617 mJ/m^2 [37] for pure bcc Fe, the τ_{CRSS}^{twin} is found to be 7050 MPa, which is considerably higher than the experimentally determined value of 170 MPa [38]. In other words, the stress required to operate the pole mechanism is very large. As a result, the occurrence of pole mechanism is very unlikely to occur in reality, and has never been substantiated experimentally. The underlying reason is related with the requirement mono-layer stacking fault formation. The creation of a mono-layer stacking fault is unlikely owing to very high magnitude of stacking fault energy in the bcc lattice (e.g. 593 mJ/m^2 for pure ferritic Fe). Furthermore, due to uni-directional nature of twinning shear [39], the roundabout sweep of the partial around the pole would also require overcoming very high energy barrier encountered in the so-called anti-twinning direction [30].

3.2 Core dissociation model (bcc)

The dissociation of a pure screw dislocation core ultimately leading to the twin formation was first proposed by Sleeswyk, Lagerlof [40, 41]. Figure 5 illustrates the process. Due to the instability of the non-planar core, a screw dislocation of $\frac{a}{2}\langle 111\rangle$ type can dissociate into three $\frac{a}{6}\langle 111\rangle$ fractional ones on the non-parallel $\{112\}$ planes. Such a configuration is stable without any applied stress. However, when the applied mechanical forces are sufficiently large, two of the fractional dislocations tend to glide to the most stressed $\{112\}$ plane. Thus, two $\frac{a}{6}\langle 111\rangle$

dislocations eventually cross-slip onto the planes parallel to the one containing the third dislocation. Continuation of applied loading results in the further gliding away of theses dislocations in the same direction, generating the adjoining stacking faults. These stacking faults separated only by one atomic layer constitute a twin embryo. The concept of twin nucleation as a result of slip dissociation is also discussed by Ogawa and Priestner [42, 43]. From the dislocation core dissociation mechanism, the τ_{CRSS}^{twin} is proposed to be $\frac{3\gamma_{isf}}{b}$. Using γ_{isf} = 593 mJ/m^2 for pure Fe, the τ_{CRSS}^{twin} is estimated to be 2500MPa for bcc Fe (compare this with the experimentally found magnitude of 170 MPa). As a result, this mechanism is also very unlikely to occur in real materials.

3.3 Pole mechanism (fcc)

While it is quite improbable that the single-pole based mechanism would ever transpire in bcc lattice, the fcc crystals with relatively low γ_{isf} are known for having stable mono-layer stacking faults. Modified versions for the pole-induced twinning process are proposed by Venables and Sleeswyk [44-46] as illustrated in Figure 6.

At the outset, there exists a pole dislocation with a long jog (blue line) from which a loop of Shockley partial of type $\frac{a}{6}\langle 112\rangle$ emits on a $\{111\}$ plane. With applied loading, the expanding glissile partial (yellow) sweep around the two poles. Due to the sweeping at two poles, portions of the expanding loop come in the close vicinity. In addition, at the same time, two new jogs (red lines) are created at both poles. The meeting ends of the sweeping partial do not intercept head-on, rather a vertical displacement of one atomic layer occurs during the glide. Meanwhile, the newly created mobile jogs serve as two new sources for two more Shockley partials in one atomic layer below and above the first one. With moving jogs (towards each other), new twining dislocations (orange and blue) expand, and undergo a similar wrap-around the pole followed by an offset of atomic layer. Now, one partial annihilates another loop, thus joining different layers of stacking fault, forming a continuous spiral. With three adjoining fault layers, a twin nucleus is formed.

3.4 Fault pair model (fcc)

Noting the experimental evidence of significant pre-twinning slip activities, Mahajan [47] proposed that deformation twins in fcc lattice would nucleate due to the interaction between fault

pairs (also known as extrinsic stacking fault). Figure 7 describes a simplified version of the model. Due to low γ_{isf}, two full dislocations of $\frac{a}{2}\langle 110\rangle$ type dissociates into two pairs of Shockley partials separated by ribbons of stacking fault (red and green) on the same $\{111\}$ twinning (or slip) plane. Interaction with other pairs of similar extended dislocations from the adjacent layer leads to the creation of two extrinsic stacking faults (i.e. two adjoining stacking fault layers). Under continued applied stress, two such fault pairs further interact with each other, whereupon mutual annihilation as well as further cross-glide results in three consecutive layers of fault planes. This assembly constitutes a twin embryo.

3.4 Atomistic shear model (fcc and bcc)

Layer by layer accumulation of stacking faults is the key to theorizing the twinning process. Such phenomenon would essentially be subjected to overcoming fault energy landscape from the discrete crystal level. As Figure 8 illustrates, the formation of an embryonic twin in a metallic lattice would encompass rigid shearing of the parent crystal (matrix), leading to the mirrored atomic arrangement. This process is aided by glissile twinning partials [48, 49].

Classically, the most important crystal-related parameter associated with twinning has been the γ_{isf}. It has been regarded for a long time that the increased twinning propensity is associated with a low γ_{isf}, for example, in fcc metals and alloys. As a result in the classical phenomenological literature [50], the parameter γ_{isf} has been used extensively as the twinnability assessment metric. However, the most recent experimental findings suggest that the γ_{isf} alone cannot fully interpret the competition between the slip versus twinning. As demonstrated in Fe-Cr and Co-Ni single crystals, the fact that either mechanism is initiated only by the maximum resolved shear stress (by varying loading/crystallographic directions) implies that the respective energy barriers must be of comparable magnitudes. To seek the answer to these experimental discoveries, theoretical calculations of twinning stresses are conducted using the γ surface first introduced by Vitek [51].

4. Atomistic fault energetics of slip and twinning

4.1 Generalized stacking fault energy (GSFE) or γ surface

Figure 9 illustrates a cutaway view of a single slip plane from the $\{111\}$ family in an fcc lattice along with the calculated the γ surface for fcc Ni-2.9%Co [52] from density functional theory (DFT) simulations. Such energy landscape can be computed from embedded atom method (EAM) based on molecular statics simulations as well. It is generally known that the DFT methods produce more accurate results. The accuracy of the EAM based calculations is a function of the relaxation schemes (e.g. full relaxation, vertical relaxation and volume relaxation) and potential itself. For example, a comparison of DFT versus EMA based predictions is performed by Chowdhury et al. [33] considering the role of composition on the intrinsic stacking fault energy in fcc Ni-Co alloys. The γ_{isf} value of pure Ni was predicted to be about 128 mJm^{-2} both from DFT [53] and EAM formalism [54]. However, DFT-predicted values for Ni-Co alloys differ significantly from the EAM values computed using two different potentials: by Zhou et al. [54] by Pun and Mishin [55].

The physical significance of such energy landscape is related with intrinsic material preference to follow the minimum energy path for lattice shearing [56]. These energy descriptions are important indicators of the competition among full/partial slip and mechanical twinning). In an fcc lattice, to calculate the entire energy landscape, two adjoining crystal blocks are rigidly sheared by an incremental displacement of $\vec{u} = \vec{u}_{\langle 110\rangle} + \vec{u}_{\langle 112\rangle}$. For a full dislocation of $\frac{a}{2}\langle 110\rangle$ type, the shear displacement, $\vec{u}_{\langle 110\rangle}$ is imposed between the two blocks. On the other hand, for a Shockley dislocation of type $\frac{a}{6}\langle 112\rangle$, the crystal is rigidly sheared along a $\langle 112\rangle$ direction by the displacement vector, $\vec{u}_{\langle 112\rangle}$. The preference of $\frac{a}{2}\langle 110\rangle$ slip over $\frac{a}{6}\langle 112\rangle$ slip can be predicted from comparing the respective peak energies [57]. The generalized stacking fault energy (GSFE) profile presented in Figure 16(a) represents an energy-displacement relationship for an extended dislocation in Co-33%Ni [52].

4.2 Generalized planar fault energy (GPFE)

The GPFE is the energy-displacement curve, which is created upon layer-by-layer shear displacement of atomic blocks [3, 57]. In Figure 10(b), the GPFE for the Co-Ni is presented as an example. Starting from a perfect fcc stacking, an intrinsic stacking fault (corresponding to an energy γ_{isf}) is first created by the shearing the crystal by one Burgers vector. The energy barrier to overcome the creation of the stacking fault is designated as the γ_{us} (the so-called unstable

stacking fault energy). The energy profile up to this point in fact corresponds to that of the GSFE. However, unlike the GSFE construction, the subsequent rigid shear (after one Burgers vector of displacement along a certain plane) is conducted on an adjacent parallel plane, which is one atomic layer above. The displacement of one Burgers vector in the neighboring layer forms a two-layer fault, which is also known as "the extrinsic stacking fault". The shear displacement by the same amount on the third consecutive layer produces a twin nucleus. Further displacement of adjoining planes adds more layers to the twin embryo, which is known as the twin migration process.

Figure 10(c) presents both the GSFE and GPFE curves for pure bcc Fe and Fe-50%Cr materials for a $\langle 111 \rangle \{112\}$ system. The energy barrier to slip (from GSFE) is considerably higher than that of twinning. However, unlike fcc twinning, bcc materials are characterized by either perfectly reflective twin or the so-called isosceles twin (which can be understood as a reflective atomic arrangement, however, slightly displaced along the boundary). It was discovered from the atomistic calculations that in pure bcc Fe the isosceles boundary corresponds to the minimum energy path while the reflective one is favored in the Fe-50%Cr.

4.3 GSFE/GPFE as indicators for preferred deformation mechanism

The relative shapes of the GSFE and GPFE curves could be used as a general indicator of which deformation mode would be favored in a pristine crystal i.e. free of grain boundaries, texture or any other source of local stress concentration [57-59]. A definitive description of deformation trend could be more physically rationalized by comparing the γ landscapes [3, 60]. Figure 11(a) illustrates various energy scenarios and their implications regarding the defect nucleation propensity in pristine fcc crystals. For the convenience of comparison, let us consider three hypothetical cases with the same magnitude of the γ_{us} but varying γ_{isf} and γ_{ut}. In a case where the γ_{isf} is considerably low and γ_{ut} is high, the plastic deformation would be characterized by dissociated slip. The lower magnitude of γ_{isf} is, the more wide the stacking fault becomes. This effect can be understood in terms of the nucleation energy barrier that the second partial of an extended dislocation would need to overcome [57]. Upon the nucleation of the leading

partial (by overcoming the energy barrier γ_{us}), the second partial has to exceed a quantity equal to ($\gamma_{us} - \gamma_{isf}$). That is to say, a large difference between γ_{isf} and γ_{us} would promote splitting of full dislocations into partials. On the same rationale, in materials where both the γ_{ut} and the γ_{isf} have high magnitudes, the plasticity would be dominated by full dislocations. The effect of high γ_{ut} corresponds to the preclusion of twinning process, while the high γ_{isf} makes the creation of stacking fault difficult. In other words, lower magnitudes of both γ_{ut} and γ_{isf} levels would favor twinning.

Similar energetic rationale could also be employed for defect nucleation in bcc lattices as presented in Figure 11(b). The γ_{isf} in bcc lattice is generally large, thus making the existence of a monolayer of stacking fault improbable. Therefore, we consider fault energy scenario with a high and constant γ_{isf}. With a considerably large γ_{us}, the mechanical twinning would be a preferred defect nucleation scenario. When the γ_{us} and the γ_{ut} levels are comparable, it is possible to have both slip and twinning. For the case when the γ_{us} is smaller, the material would tend to deform via slip only. Table 1 lists a compilation of DFT and experimental data on the parameters g_{isf}, γ_{us} and g_{ut} (from [61]).

5. Prediction of critical stresses related to deformation twinning

5.1 Earlier theories on twin nucleation

It is now accepted that deformation twinning occurs via a succession of Shockley partials on adjacent planes. Consecutive shearing of lattice first creates an intrinsic stacking fault, then an extrinsic one (i.e. a two-layer fault), and finally a three-layer twin. After the nucleation of the twin embryo, the subsequent gliding results in the twin migration process. These considerations are reflected in numerous twin nucleation models in the earlier literature. On phenomenological grounds, significant recent theoretical progresses are made [62, 63]. Mechanistically, a number of researches earlier were geared at predicting twinning stress.

Venables [64] predicted the critical twin nucleation stress founded on the overcoming of frictional resistance to generate an intrinsic stacking fault. Afterwards, Pirouz [65] considered the motions of a leading and a trailing partial dislocation bound by a stacking fault. Moreover,

Miura et al. [66] introduced an extrinsic stacking fault as a condition for the nucleation of a twin embryo. Karaman et al. [50] built on these very ideas and extended to modeling solute effects on the twinning stress. Extensive Eshelby type analyses were undertaken by Meyers et al. [67]. Consequently, there were able to incorporate deformation kinetics considerations (i.e. strain-rate, temperature etc.). We note that all these theories are essentially took into account the role of intrinsic stacking fault energy (γ_{isf}) as the primary material input for predicting twinning stress.

Fischer et al. [68] formulated twinning stress based on thermodynamics based energy balance. This approach took note of the geometrical considerations such as arrangement of dislocations. The need for incorporating atomistic energetics was brought into attention by Tadmor and co-workers [59, 69]. They demonstrated that material twinnability (via a case study in fcc materials) can evaluated with the aid of fault energies, i.e. γ_{isf}, γ_{us} and γ_{ut}. It was evident from their work that the unstable energies (γ_{us} and γ_{ut}) are equally crucial to establish a comprehensive twinning criterion along with more traditionally used γ_{isf}. Now, twin nucleation, according to these models, is triggered by the presence of a sufficiently high local stress concentration source (e.g. dislocation pile-up [64], Lomer-Cottrell barrier [50, 65], grain boundary [66], dislocation wall [68], micro-crack [59]). Twin nucleation propensity in the bulk of the material would indicate the inherent material propensity for such deformation mechanism. In the regard, the recent developments on the utilization of GSFE or GPFE curves are worth mentioning. For instance, Kibey at al. [70] proposed a closed-form equation for the twinning stress prediction, which utilized DFT-computed GPFE levels both in elemental metals and alloys. Thus, intricate effects of interactions between substitutional solutes and host atoms such as the so-called Suzuki segregation (discussed later) were captured.

5.2 Recent models on twin nucleation

Recent models for predicting twin nucleation stress in bulk crystal configuration (i.e. in absence of any source as mentioned earlier) utilized the atomistic γ surfaces [52, 71]. These approaches consider the fundamental Peierls-Nabarro based assumptions of slip disregistry (i.e. elastic distortion caused by the presence of slip) [72, 73]. [74, 75]. Such an approach inherently permits the considerations of slip, intrinsic/extrinsic stacking fault generation prior to twin formation. The fundamental premise for predicting CRSS for twin nucleation (τ_{CRSS}^{twin}) is that the applied mechanical work ought to overcome the total energy expenditure as in Equation (1):

$$\underbrace{td\varepsilon_{twin}\tau_{CRSS}^{twin}}_{\text{applied work}} = \underbrace{E_{interaction}+E_{GPFE-nucleation}}_{\text{energy cost}} \quad (1)$$

where, t, d and ε_{twin} are twin thickness, length and shear strain respectively. Typically, the relationship, $d \approx 10t$, is considered for an embryonic twin [76, 77]. The elastic interaction energy ($E_{interaction}$) among twinning dislocations can be obtained from classical formulations as follows [78].

$$E_{interaction} = \frac{\mu b_{twin}^2}{4\pi(1-\upsilon)}\left(\ln\frac{D}{d_{1-2}}+\ln\frac{D}{d_{2-3}}+\ln\frac{D}{d_{1-3}}\right) \quad (2)$$

Where, D is the single crystal size; μ is the shear modulus, d_{1-2} distance between dislocation "1" and "2". The spacings among the twinning dislocations are: $d_{1-3}=\frac{\mu b_{twin}^2}{2\pi\gamma_{isf}}$, $d_{2-3}=0.732d_{1-3}$ and $d_{1-2}=d_{1-3}-d_{2-3}$ upon balancing the acting elastic forces [41]. The term $E_{GPFE-nucleation}$ represents the area underneath the GPFE curve corresponding the portion of twin nucleation. Equation (1) can be solved for τ_{CRSS}^{twin}. Thus predicted results on several bcc materials are compared with the experimental values (pure bcc Fe, Fe-3%V, Fe-50%Cr and Fe-25%Ni) in Table 2(a) [71]. The predicted levels of τ_{CRSS}^{twin} fcc Co-Ni alloys are presented on Table 2(b).

For the case of a pre-existent dislocaiton arrangement present in the vicinity, the movement of an approaching twin nucleus would be restricted (Figure 12). Slip-twin interaction may lead to twin migration process which is the growth or shrinkage of a pre-existent twin after the embryonic twin is nucleated [7, 79]. Elastic properties of dislocation arrays (i.e. their interaction with approaching dislocations) have been studied extensively by Li and co-workers [80-82]. Building on these foundations, a recent model [52] included the GPFE considerations and predicted $\tau_{CRSS}^{twin-slip}$ with accuracy. As sketched in Figure 12, such a problem essentially involves interactions among the twinning slip (i = 1, 2 and 3) and the "wall" of dislocation dipoles (j = 1, 2, 3, … N_{dipole}).

The consideration of dipole array is rationalized on the basis of energetic stability of the configuration as established earlier by Neumann [83]. The amount of applied work, $W_{applied} = td\varepsilon_{twin}\tau_{CRSS}^{twin-slip}$ needs to overcome the total energy expense: (i) the interaction among the wall and the twinning dislocations ($E_{twin\text{-}wall\ interaction}$) and (ii) the atomistic shear ($E_{GPFE-migration}$). An expression similar to Equation (1) can be derived and solved for $\tau_{CRSS}^{twin-slip}$. The term $E_{twin\text{-}wall\ interaction}$ is evaluated in a similar manner as in Equation (2). The $E_{GPFE-migration}$ represents the area underneath the GPFE curve corresponding to the migration portion. The predicted level of twin-slip interaction ($\tau_{CRSS}^{twin-slip}$) for fcc Co-Ni alloys are presented in Table 2(b). A comparison is made with a single slip nucleation stress (τ_{CRSS}^{twin}) and (τ_{CRSS}^{slip}) and the associated experimental magnitudes.

6 Annealing twins and associated modeling

6.1 Nanotwinned Microstructure

Experimental reports [84, 85] noted the superior strength and ductility of metallic materials rife with nano-sized annealing twins (i.e. the pre-existent ones). Given the limitations of the experimental techniques to capture the physical processes at the nanoscale, these findings prompted various non-continuum modeling approaches such as molecular dynamics simulations [23, 27, 86]. From a mesoscale perspective, the role of annealing twins on macroscopic mechanical behavior has been also addressed on the ground of deformation kinetics principles [87, 88]. The primary effect of introducing stable nanotwins in the material microstructure is found to sub-divide host grains, leading to a markedly decreased activation volume (on the order of several b^3 ; b being the Burgers vector) for a refined microstructure [89, 90]. For conventional coarse-grained material, the activation volume is typically on the order of >1000b^3. Intuitively, a greater degree of applied shear stress would be required to initiate and sustain plastic flow in a microstructural environment non-conducive to widespread slip. As a result, the critical resolved shear stress (hence, macroscale yield strength) would be considerably enhanced. It has been suggested that a wide variation in the slip transfer mechanisms past a coherent twin boundary plays a significant role in dictating toughness.

6.2 Slip transfer mechanisms past coherent twin boundaries

The nature of various slip-twin boundary interception outcomes in fcc crystals has been scrutinized rigorously in the literature using experimental techniques [19, 22, 30, 91, 92], and also with theoretical treatments [26, 27, 93-96]. The important roles of individual mechanisms on the hardening behavior of fcc metals and alloys have been predicted elaborately. These treatments bring into attention the promise of considering different strain transfer mechanisms across the interface into a comprehensive deformation theory for nano-twinned materials. The occurrence of various slip-coherent twin boundary reactions is found to be strongly dependent on the relative Schmid factors on the twin boundary, incident, and outgoing slip systems [97]. Five most commonly observed slip transfer mechanisms past a twin boundary are: (a) incorporation, (b) transmission, (c) multiplication, (d) transmission and incorporation and (e) blockage by a Lomer lock formation. Molecular dynamics studies of these reactions by various researchers are presented in Figure 13 (from [23, 25, 27, 94, 98]).

The impinging slip results in incorporation upon the boundary, provided the relative Schmid factor on the interface is very high (i.e. a situation conducive to a twin migration process) [26, 27, 99]. It is important to note that even though an incorporation process can be deemed as an effective blockage mechanism for oncoming slip, it does not preclude the incorporated slip continuing in a glissile motion on the twin boundary, resulting in twin growth/shrinkage [100]. On the other hand, direct transmission [22, 23] occurs when the slip systems inside the twinned crystal experience relatively high Schmid factors. Multiplication of slip [28] at the interception site transpires when the incident and the outgoing slip systems are activated with similar Schmid factors. A combination of both

incorporation and transmission events [92, 101, 102] arises under a comparable incident/outgoing stress state, however, along with a high Schmid factor on the twin boundary. Nucleation of a Lomer lock in conjunction with a stair rod dislocation [24, 25] occurs when the resolved shear stresses on incident/outgoing/boundary slip systems are all rather low. We note the fundamental difference between dislocation blockage due to incorporation (which allows continuous straining on the interface) and a Lomer lock (which precludes any glissile activity until further incidence breaks the lock). It is interesting that two of the aforementioned slip transfer mechanisms promote continuation of local straining on the interface (i.e. contribute to the twin migration process). Early literature [23] notes that the origin of considerable ductility in nano-twinned materials can be attributed to the pervasive incorporation process. We note that the most unique signature of these reaction mechanisms is the magnitude of the residual dislocation (b_r) left onto the twin boundary following the impingement.

6.3 Significance of reaction-specific γ_{us} and b_r at a twin boundary

It is intuitive that the magnitudes of the energy barrier to slip (i.e. γ_{us}) would differ to considerable extents for the individual slip transfer mechanisms. In order to compute the γ_{us} for various reactions, the "tracing atoms" method can be used in molecular dynamics simulations. As in Figure 14, the potential energy of the tracing atoms ahead of an oncoming slip are constantly monitored. The differential between bulk and the slip-influenced potential energy, $\Delta E = E - E_{bulk}$ is computed as the slip approaches [94, 103]. The insets show the position of the extended dislocation with respect to the tracing atoms, and the corresponding γ levels which is equal to the ratio, $\Delta E / w\ell$ after Vitek [51]. The dimensions of the tracing atomic area (w times ℓ) are chosen judiciously to ensure convergence of the γ energy which occurs at larger ℓ and smaller w (Figure 14) [104].

Using such method, [94] computed the entire GSFE curve specific to a slip-twin boundary reaction (Figure 15) in Cu. They considered the incidence of a single dislocation upon a coherent twin boundary in the molecular dynamics simulations. It follows from their findings that the formation of Lomer lock requires overcoming the maximum energy barrier while the incorporation process has the lowest. Subsequently, [52, 103, 105] determined the evolution of b_r as well as γ_{us} with respect to multiple slip incidence on the boundary (Figure 16).

The saturation in the γ_{us} was attributed to the b_r achieving a steady-state magnitude with increasing incidence of slip. The origin of the saturation effect for individual case is related with precipitous rise in the local stress concentration (due to gradual accumulation of b_r) at the reaction site upon successive slip impingement. The details of b_r saturation mechanism with respect to gradual slip incidence differ from case to case; however, the fundamental mechanistic process is essentially similar. With increasing pile-up stress from the oncoming slip, the accumulated b_r eventually breaks down into multiple glissile and/or sessile slip at incidence site. With sufficiently large of approaching slip, the magnitude of br eventually reaches a point where a stable pattern of residual slip dissociation occurs. In the process, new glissile dislocation glide away leaving behind the b_r of the saturated magnitude. The correlations among the γ_{us}, br and number of incident slip (n_{slip}) as in Figure 16 provide invaluable

energetic perspectives into the relative penetration resistances of the various strain transfer mechanisms.

The ref [106] and [107] modeled bcc twin-twin interaction using similar molecular dynamics simulations in Nb. Further details of the interaction mechanism between an annealing twin and a propagating one in bcc Fe-Cr lattice is investigated by [71]. Under $[0\bar{1}0]$ tensile loading (farfield), an incoming twin consisting of three fractional dislocations of type $\frac{a}{6}\langle 111\rangle$ impinges on the existing twin boundary as presented in Figure 17. The ensuing process involves the incorporation of the approaching twinning partials onto the twin boundary leaving a residual dislocation with Burgers vector, $\vec{b}_r$ (of magnitude equal to 1.0a). A compressive load along the $[111]$ crystallographic direction results in a similar incorporate process, however, with a different b_r (equal to 0.82a). The apparent different outcomes for tension and compression cases can be attributed to the differences in the levels of Schmid factors on the activated systems.

6.4 Predicting friction stresses for twin-slip or twin-twin reactions

The frictional stress specific to any reaction outcome of slip intercepting a twin ($\tau_{CRSS}^{reaction}$) in presence of $\vec{b}_r$ can be predicted by considering two distinct forms of energy contributions: (a) the extrinsic level of fault energy subjected to local stresses, $E_{GSFE/GPFE}$ (note that GPFE is applicable for incorporation process only) and (b) the residual elastic energy due to $\vec{b}_r$, $E_{residual} = E_{residual}(b_r)$ [33]. The applied stress $\tau_{CRSS}^{reaction}$ required to move an oncoming dislocation towards the boundary by a distance of ∂d is derived based on the work-energy balance as follows.

$$\underbrace{b_{incident}\tau_{CRSS}^{reaction}\partial d}_{work\ done} = \underbrace{\partial E_{GSFE/GPFE}\left(f_{disregistry},\gamma\right)+\partial E\left(b_r\right)}_{energy\ expense} \quad (3)$$

The predicted stresses using Equation (3) in fcc Ni-Co alloy is presented in Table 3 (also Figure 16). Similarly, in bcc materials, the $\tau_{CRSS}^{twin-twin}$ is predicted and compared with experimental values based on single-crystal studies as in Figure 18 [71].

To predict the τ_{CRSS}^{poly} for the polycrystalline nano-twinned Ni-Co alloys, three major flow contributions are considered: (a) the free glide stress $\tau_{free\ glide}$, (b) slip-twin boundary interaction stress, $\tau_{CRSS}^{reaction}$, and (c) the forest hardening stress (at a pre-deformation dislocation density) $\tau_{forest} = \alpha\mu b\sqrt{\rho}$ [108, 109]; where α is a material constant (from 0.5 to 1) and ρ the forest dislocation density (assumed to be 10^{14} /m^2 which is the typical pre-deformation literature value). The $\tau_{CRSS}^{reaction}$ is observed to be the most dominating. Using Equation (4), we calculate the τ_{CRSS}^{poly} levels for different Ni-Co alloys based on iso-strain type mixing formulations.

$$\tau_{CRSS}^{poly} = (1 - V_f)\tau_{free\ glide} + \sum_{reaction} V_f^{reaction}\tau_{slip\text{-}twin}^{reaction} + (1 - V_f)\tau_{forest} \quad (4)$$

where, V_f is the total volume fraction of the material region hosting the aggregate slip-twin reactions; $V_f^{reaction}$ is the assigned volume fraction for a specific reaction i.e. $V_f = \sum_{reaction} V_f^{reaction}$.

The predicted CRSS for polycrystalline Ni-Co alloys are compared in Figure 19with experimental ones (determined by using Taylor factor normalization for the uniaxial stress-strain data in Figure 2(c)).

7. Further problems: polycrystalline deformation, fracture behavior, phase transformation, hcp deformation

The foregoing models have examined the single crystal behavior without the presence of multiple grains. It is important to characterize single crystals to understand polycrystalline deformation, in that they provide insight into inherent defect evolution circumventing the effects of texture and interfaces. The plastic stress-strain behaviors of single crystals consist of three mechanistically distinct hardening regimes such as stage I, II and III [110-112]. The initial plasticity (stage I) is dominated by massive defect nucleation (e.g. slip or twin) followed by the ensuing hardening stages characterized by more complex defect interplays. For example, the fluctuating nature of the flow is more pronounced in bcc than in fcc [30]. This could be attributed to the considerable difference in the energy barriers between twin nucleation and migration in bcc than fcc materials. These trends may be subjected to significant modifications due to the presence of material interfaces. In a multi-grain environment, the presence of grain boundaries would considerably affect the overall material behaviors. The role of interfaces as obstacles to flow and/or sources of defect nucleation would give rise to different macroscale constitutive

responses. For example, upon studying polycrystalline Co-33%Ni with low stacking fault energy, Remy [8] attributed the increased hardening response to the slip obstruction due to an abundance of newly generated twin boundaries. It was argued that extensive twinning sub-divides a particular grain in multiple segments restricting the slip mobility, therefore, giving rise to Hall-Petch type strengthening effects. In general, conventional fcc single crystals shows twinning behavior only at very high stress [113, 114] and strain-rate. From a continuum standpoint, [67] utilized Eshelby type analysis to theorize the strain-rate, temperature effects on twinning. Similarly, in molecular dynamics based simulations with high strain-rate, many researchers investigated the mechanistic aspect of deformation in nanocrystalline multi-grain configurations.

Yamakov et al. [115] considered the deformation behaviors of Al multi-grained structure (Figure 20) with an average grain diameter of 70 nanometers. Deformation twins are found to form at the grain boundaries. The mechanism is initiated in the form of a single partial dislocation nucleation followed by parallel and adjacent slip. Consecutive gliding of Shockley partials eventually result in a deformation twin. Similarly, Shabib and Miller uncovered the nucleation of extended stacking fault generation aided by gliding of Shockley partial dislocation, which originated at a grain boundary [116]. In an different approach, [117, 118] studied Cu polycrystalline structures with inherent annealing twins of nanometer size. Two distinct mechanistic trends were observed as a function of twin spacing. For thinner twins (of 1.62 nm), slip nucleated parallel to the twin boundaries with no significant hardening contribution from the presence of twins. On the other hand, when the twin spacing was about 6 nm slip crisscrossed the grain and intercepted the twin boundaries giving rise to significant hardening. Upon sufficient deformation, massive slip nucleation occurs from the grain boundaries, which intercept the twins. These studies have provided important mechanistic understanding of twinning-based deformation in nanocrystalline microstructure. Energetic representation of polycrystalline deformation poses, as we envision, a promising future endeavor, which would further reveal the relative strengths of, say, various interface types, defect interaction etc. for polycrystal deformation.

Another interesting and important application of the atomistic aspects of plasticity lies in understanding crack propagation behavior, which is a significant engineering concern in a wide range of materials [6, 105, 119, 120]. Damage response under static or cyclic loading is decided by the irreversible plastic phenomena at the cracktip in the form of slip or twinning. Earlier Rice and co-workers [121, 122] established the importance of atomistic description of cracktip

behavior. In particular, their analysis highlighted the use of the unstable stacking fault energy γ_{us} in the context of modeling cracking behavior. Subsequently, Tadmor and co-workers [59, 69] conceptualized the twinnability in front of a propagating crack considering a comprehensive treatment of fault energy parameters (i.e. γ_{isf}, γ_{us} and γ_{ut}). They demonstrated that density functional theory based fault energy parameters can be used to predict twinning propensity for mesoscale crack propagation. This is a significant advancement in the modeling of crack behaviors, in that they pave the way for further advancing crack modeling using atomistically computed γ surface. On molecular dynamics frontier, there have been significant progresses on fracture behaviors as well. One of the earlier studies of twinning-mediated crack propagation using molecular dynamics simulations was undertaken by [123]. In their work, the critical stress intensity factor was established on the basis of atomistically sharp crack advancing via twinning in copper. More recently, using molecular dynamics modeling, [60] study the completion of twinning with slip at a crack-tip. They proposed that the relative size/shape of GSFE/GPFE curves would strongly dictate one plastic mechanism (e.g. twinning) over another (e.g. slip). Founded on these works, recent modeling efforts [124, 125] have noted the incorporation of the atomistically predicted slip glide strengths into a formalism to predict cyclic damage metrics. Similarly, the friction stresses for twinning mechanism also hold considerable promise for theorizing the crack advancement problem. For materials which predominantly deform via twinning (e.g. hcp metals and alloys), such modeling can shed new light in terms of physical mechanism(s) of cracking [126]. For the readers benefit, a summary of relevant works discussed in the paper is provided in Table 4.

Atomistic modeling can also benefit the area of phase transformation materials such as the shape memory alloys behaviors [127-131]. For instance, the shape memory alloys (e.g. NiTi) undergo martensitic phase transformation, which is also accompanied by deformation twinning. In the last decade, a number of molecular dynamics based studies have emerged depicting the twinning phenomena [132-134] in shape recovering alloys. A comprehensive GSFE or GPFE based analysis there could be particularly useful to understand materials deformation predilection such as competition among slip, twining and transformation phenomena [135]. Similarly, metallic materials with hexagonal close packed (hcp) lattice undergo twinning dominated plasticity [136, 137], which can benefit from atomistic energetics modeling [138].

8. Appropriate use of atomistics and modeling larger-scale deformation

One ought to account for the uncertainty of the calculations while employing atomistic quantities to derive continuum models. Applicable to both MD and DFT based energy calculations is the sensitivity of: (i) the method adopted for atomic relaxation and (ii) simulation supercell size. Atomic positions can be allowed to adjust all x, y and z coordinates (full relaxation) or the adjustments can occur only in the direction vertical to the fault plane (partial relaxation). It is important to note that the empirical potential based fault energies can be particularly sensitive to the choice of relaxation scheme [139, 140]. One reasonable method of validating empirical potential obtained calculations would be to compare them density functional theory calculations, which are considerably less susceptible to such artifacts. One should also be careful regarding the simulation supercell size as well as the boundary conditions. For instance, the number of layers in the direction vertical to the glide plane considered during the rigid shear simulations needs to large enough to reach energetic convergence. To simulate bulk properties in molecular dynamics, the system size ought to be sufficiently large such that physical observables (i.e. the total energy, entropy) converge regardless of further increase in the supercell volume. This can be established by conducting multiple simulations with varying dimensions (x, y and z) of representative volume element. Once the correct level of convergence of atomistic parameters is ascertained, their incorporation into the prediction of continuum-scale CRSS levels would lead to better agreement with the experimental values. Another concern of importance is the introduction of non-systematic error in DFT calculations. For example, the small errors in lattice constant of the defect plane can move since the inter-planar spacing is a function of lattice constant, a small error in the lattice constant magnitude can lead to over- or under-estimation of atomic distances. One possible way to eliminate accumulation of such errors is the usage of average experimental lattice constant in establishing the large deformation cell while permitting local relaxations [141].

From modeling standpoint, the CRSS levels represent the initial stage of plasticity i.e. immediately following the elastic deformation. The macroscopic yielding of materials is primarily decided by overcoming the critical resolved shear stresses at the microscale. Hence, it is reasonable and sufficient to consider only the lattice friction resistance. Evidently, the scope of such approach does not yet address the entire spectrum of the material stress-strain behavior particularly the aspect of massive defect evolution. The current lengthscales associated with atomistic modeling is confined to nanometers. However, the post-yield deformation mechanics would be primarily governed by extensive defect interactions, the exact nature of which nature will decide the macroscopic flow behavior. The strengthening attributes during the dynamic

evolution of defects are large decided by the complex assortment of plastic mechanisms. As promising future refinement in modeling efforts, the development of a combined atomistic and mesoscopic modeling platform would serve such a need. For instance, the discrete lattice effects need to be bridged via extensive mesoscale defect modeling (e.g. dislocation dynamics) [142] [143, 144] and/or deformation kinetics [145]. It should be noted that the models address within atomistic framework do not incorporate the role of thermal and rate-dependent phenomena. In order to address the temperature and strain-rate effects, the atomistic theory could be modified with the principles of the deformation kinetics [145, 146]. The plastic flow mechanisms that are dependent on the deformation rate/temperature abide by the Arrhenius laws, which dictate an exponential dependence on an energy barrier to be overcome. In that regard, the current calculations consider the efficacy of the unstable stacking fault energy, γ_{us}, being the most deciding energy barrier parameter to quantify the resistance to plastic flow.

9. Acknowledgement

The financial supports from the Nyquist chair funds are acknowledged.

References

[1] Tucker, G. J., and Foiles, S. M., 2015, "Quantifying the influence of twin boundaries on the deformation of nanocrystalline copper using atomistic simulations," International Journal of Plasticity, 65, pp. 191-205.
[2] Li, J., Ngan, A. H., and Gumbsch, P., 2003, "Atomistic modeling of mechanical behavior," Acta Materialia, 51(19), pp. 5711-5742.
[3] Ogata, S., Li, J., and Yip, S., 2005, "Energy landscape of deformation twinning in bcc and fcc metals," Physical Review B, 71(22), p. 224102.
[4] Ogata, S., Li, J., and Yip, S., 2002, "Ideal pure shear strength of aluminum and copper," Science, 298(5594), pp. 807-811.
[5] Jin, Z. H., Dunham, S. T., Gleiter, H., Hahn, H., and Gumbsch, P., 2011, "A universal scaling of planar fault energy barriers in face-centered cubic metals," Scripta Materialia, 64(7), pp. 605-608.
[6] Chowdhury, P., and Sehitoglu, H., 2016, "Mechanisms of fatigue crack growth–a critical digest of theoretical developments," Fatigue & Fracture of Engineering Materials & Structures.
[7] Remy, L., 1977, "Twin-twin interaction in FCC crystals," Scripta Metallurgica, 11(3), pp. 169-172.
[8] Remy, L., 1978, "Kinetics of fcc deformation twinning and its relationship to stress-strain behaviour," Acta Metallurgica, 26(3), pp. 443-451.
[9] McPhie, M., Berbenni, S., and Cherkaoui, M., 2012, "Activation energy for nucleation of partial dislocation from grain boundaries," Computational Materials Science, 62, pp. 169-174.
[10] Warner, D. H., Sansoz, F., and Molinari, J. F., 2006, "Atomistic based continuum investigation of plastic deformation in nanocrystalline copper," International Journal of Plasticity, 22(4), pp. 754-774.
[11] M'Guil, S., Wen, W., Ahzi, S., Gracio, J. J., and Davies, R. W., 2015, "Analysis of shear deformation by slip and twinning in low and high/medium stacking fault energy fcc metals using the ϕ-model," International Journal of Plasticity, 68, pp. 132-149.
[12] Sun, C. Y., Guo, N., Fu, M. W., and Wang, S. W., 2016, "Modeling of slip, twinning and transformation induced plastic deformation for TWIP steel based on crystal plasticity," International Journal of Plasticity, 76, pp. 186-212.
[13] Müllner, P., and Romanov, A., 2000, "Internal twinning in deformation twinning," Acta materialia, 48(9), pp. 2323-2337.

[14] Tadmor, E. B., and Miller, R. E., 2011, Modeling materials: continuum, atomistic and multiscale techniques, Cambridge University Press.
[15] Jo, M., Koo, Y. M., Lee, B.-J., Johansson, B., Vitos, L., and Kwon, S. K., 2014, "Theory for plasticity of face-centered cubic metals," Proceedings of the National Academy of Sciences, 111(18), pp. 6560-6565.
[16] Li, W., Lu, S., Hu, Q.-M., Kwon, S. K., Johansson, B., and Vitos, L., 2014, "Generalized stacking fault energies of alloys," Journal of Physics: Condensed Matter, 26(26), p. 265005.
[17] Lebensohn, R., and Tomé, C., 1993, "A self-consistent anisotropic approach for the simulation of plastic deformation and texture development of polycrystals: application to zirconium alloys," Acta metallurgica et materialia, 41(9), pp. 2611-2624.
[18] Chowdhury, P. B., 2016, "Modeling mechanical properties–linking atomistics to continuum," University of Illinois at Urbana-Champaign.
[19] Remy, L., 1981, "The interaction between slip and twinning systems and the influence of twinning on the mechanical behavior of fcc metals and alloys," Metallurgical Transactions A, 12(3), pp. 387-408.
[20] Wang, J., Anderoglu, O., Hirth, J. P., Misra, A., and Zhang, X., 2009, "Dislocation structures of S3 {112} twin boundaries in face centered cubic metals," Appl. Phys. Lett, 95(2), p. 021908.
[21] Sutton, A. P., and Balluffi, R. W., 1995, "Interfaces in crystalline materials."
[22] Kacher, J., Eftink, B., Cui, B., and Robertson, I., 2014, "Dislocation interactions with grain boundaries," Current Opinion in Solid State and Materials Science, 18(4), pp. 227-243.
[23] Zhu, T., Li, J., Samanta, A., Kim, H. G., and Suresh, S., 2007, "Interfacial plasticity governs strain rate sensitivity and ductility in nanostructured metals," Proceedings of the National Academy of Sciences, 104(9), pp. 3031-3036.
[24] Karnthaler, H., 1978, "The study of glide on {001} planes in fcc metals deformed at room temperature," Philosophical Magazine A, 38(2), pp. 141-156.
[25] Wang, J., and Huang, H., 2006, "Novel deformation mechanism of twinned nanowires," Applied physics letters, 88(20), p. 203112.
[26] Asaro, R. J., and Kulkarni, Y., 2008, "Are rate sensitivity and strength effected by cross-slip in nano-twinned fcc metals," Scripta Materialia, 58(5), pp. 389-392.
[27] Jin, Z.-H., Gumbsch, P., Ma, E., Albe, K., Lu, K., Hahn, H., and Gleiter, H., 2006, "The interaction mechanism of screw dislocations with coherent twin boundaries in different face-centred cubic metals," Scripta Materialia, 54(6), pp. 1163-1168.
[28] Miller, B., Fenske, J., Su, D., Li, C.-M., Dougherty, L., and Robertson, I. M., "Grain Boundary Responses to Local and Applied Stress: An In Situ TEM Deformation Study," Proc. MRS Proceedings, Cambridge Univ Press, pp. 0976-EE0902-0901.
[29] Frenkel, D., and Smit, B., 2001, Understanding molecular simulation: from algorithms to applications, Academic press.
[30] Christian, J. W., and Mahajan, S., 1995, "Deformation twinning," Progress in materials science, 39(1), pp. 1-157.
[31] Beyerlein, I. J., Zhang, X., and Misra, A., 2014, "Growth twins and deformation twins in metals," Annual Review of Materials Research, 44, pp. 329-363.
[32] Zhu, Y. T., Liao, X., and Wu, X., 2012, "Deformation twinning in nanocrystalline materials," Progress in Materials Science, 57(1), pp. 1-62.
[33] Chowdhury, P., Sehitoglu, H., Maier, H., and Rateick, R., 2015, "Strength prediction in NiCo alloys–the role of composition and nanotwins," Int. J. Plasticity.
[34] Patriarca, L., Abuzaid, W., Sehitoglu, H., Maier, H. J., and Chumlyakov, Y., 2013, "Twin nucleation and migration in FeCr single crystals," Materials Characterization, 75, pp. 165-175.
[35] Patriarca, L., Abuzaid, W., Sehitoglu, H., and Maier, H. J., 2013, "Slip transmission in bcc FeCr polycrystal," Materials science and engineering: a, 588, pp. 308-317.
[36] Cottrell, A., and Bilby, B., 1951, "LX. A mechanism for the growth of deformation twins in crystals," The London, Edinburgh, and Dublin Philosophical Magazine and Journal of Science, 42(329), pp. 573-581.
[37] Li, S., Ding, X., Deng, J., Lookman, T., Li, J., Ren, X., Sun, J., and Saxena, A., 2010, "Superelasticity in bcc nanowires by a reversible twinning mechanism," Physical Review B, 82(20), p. 205435.
[38] Harding, J., "The yield and fracture behaviour of high-purity iron single crystals at high rates crystals at high rates of strain," Proc. Proceedings of the Royal Society of London A: Mathematical, Physical and Engineering Sciences, The Royal Society, pp. 464-490.

[39] Kibey, S., Liu, J., Johnson, D., and Sehitoglu, H., 2007, "Energy pathways and directionality in deformation twinning," Applied Physics Letters, 91(18), p. 181916.
[40] Lagerlöf, K., 1993, "On deformation twinning in bcc metals," Acta metallurgica et materialia, 41(7), pp. 2143-2151.
[41] Sleeswyk, A., 1963, "½< 111> screw dislocations and the nucleation of {112}< 111> twins in the bcc lattice," Philosophical Magazine, 8(93), pp. 1467-1486.
[42] Ogawa, K., 1965, "Edge dislocations dissociated in {112} planes and twinning mechanism of bcc metals," Philosophical Magazine, 11(110), pp. 217-233.
[43] Priestner, R., and Leslie, W., 1965, "Nucleation of deformation twins at slip plane intersections in BCC metals," Philosophical Magazine, 11(113), pp. 895-916.
[44] Venables, J., 1961, "Deformation twinning in face-centred cubic metals," Philosophical magazine, 6(63), pp. 379-396.
[45] Venables, J., 1974, "On dislocation pole models for twinning," Philosophical Magazine, 30(5), pp. 1165-1169.
[46] Sleeswyk, A., 1974, "Perfect dislocation pole models for twinning in the fcc and bcc lattices," Philosophical Magazine, 29(2), pp. 407-421.
[47] Mahajan, S., and Chin, G., 1973, "Formation of deformation twins in fcc crystals," Acta metallurgica, 21(10), pp. 1353-1363.
[48] Blewitt, T., Coltman, R., and Redman, J., 1957, "Low- Temperature Deformation of Copper Single Crystals," Journal of Applied Physics, 28(6), pp. 651-660.
[49] Jin, Z., and Bieler, T. R., 1995, "An in-situ observation of mechanical twin nucleation and propagation in TiAl," Philosophical Magazine A, 71(5), pp. 925-947.
[50] Karaman, I., Sehitoglu, H., Gall, K., Chumlyakov, Y., and Maier, H., 2000, "Deformation of single crystal Hadfield steel by twinning and slip," Acta materialia, 48(6), pp. 1345-1359.
[51] Vitek, V., 1968, "Intrinsic stacking faults in body-centred cubic crystals," Philosophical Magazine, 18(154), pp. 773-786.
[52] Chowdhury, P., Sehitoglu, H., Abuzaid, W., and Maier, H., 2015, "Mechanical response of low stacking fault energy Co–Ni alloys–Continuum, mesoscopic and atomic level treatments," International Journal of Plasticity, 71, pp. 32-61.
[53] Chandran, M., and Sondhi, S., 2011, "First-principle calculation of stacking fault energies in Ni and Ni-Co alloy," Journal of Applied Physics, 109(10), p. 103525.
[54] Zhou, X., Johnson, R., and Wadley, H., 2004, "Misfit-energy-increasing dislocations in vapor-deposited CoFe/NiFe multilayers," Physical Review B, 69(14), p. 144113.
[55] Pun, G. P., and Mishin, Y., 2012, "Embedded-atom potential for hcp and fcc cobalt," Physical Review B, 86(13), p. 134116.
[56] Siegel, D. J., 2005, "Generalized stacking fault energies, ductilities, and twinnabilities of Ni and selected Ni alloys," Applied Physics Letters, 87(12), pp. 121901-121901.
[57] Van Swygenhoven, H., Derlet, P., and Frøseth, A., 2004, "Stacking fault energies and slip in nanocrystalline metals," Nature materials, 3(6), pp. 399-403.
[58] Cai, T., Zhang, Z. J., Zhang, P., Yang, J. B., and Zhang, Z. F., 2014, "Competition between slip and twinning in face-centered cubic metals," Journal of Applied Physics, 116(16), p. 163512.
[59] Tadmor, E., and Bernstein, N., 2004, "A first-principles measure for the twinnability of FCC metals," Journal of the Mechanics and Physics of Solids, 52(11), pp. 2507-2519.
[60] Warner, D. H., Curtin, W. A., and Qu, S., 2007, "Rate dependence of crack-tip processes predicts twinning trends in fcc metals," Nature materials, 6(11), pp. 876-881.
[61] Kibey, S. A., 2007, Mesoscale models for stacking faults, deformation twins and martensitic transformations: linking atomistics to continuum.
[62] Kalidindi, S. R., 1998, "Incorporation of deformation twinning in crystal plasticity models," Journal of the Mechanics and Physics of Solids, 46(2), pp. 267-290.
[63] Staroselsky, A., and Anand, L., 1998, "Inelastic deformation of polycrystalline face centered cubic materials by slip and twinning," Journal of the Mechanics and Physics of Solids, 46(4), pp. 671-696.
[64] Venables, J., 1964, "The nucleation and propagation of deformation twins," Journal of Physics and Chemistry of Solids, 25(7), pp. 693-700.
[65] Pirouz, P., 1989, "On twinning and polymorphic transformations in compound semiconductors," Scripta metallurgica, 23(3), pp. 401-406.

[66] Miura, S., Takamura, J., and Narita, N., "Orientation dependence of flow stress for twinning in silver crystals," Proc. Transactions of the Japan Institute of Metals, JAPAN INST METALS AOBA ARAMAKI, SENDAI 980, JAPAN, pp. 555-&.
[67] Meyers, M., Vöhringer, O., and Lubarda, V., 2001, "The onset of twinning in metals: a constitutive description," Acta materialia, 49(19), pp. 4025-4039.
[68] Fischer, F., Appel, F., and Clemens, H., 2003, "A thermodynamical model for the nucleation of mechanical twins in TiAl," Acta materialia, 51(5), pp. 1249-1260.
[69] Tadmor, E., and Hai, S., 2003, "A Peierls criterion for the onset of deformation twinning at a crack tip," Journal of the Mechanics and Physics of Solids, 51(5), pp. 765-793.
[70] Kibey, S. A., Wang, L.-L., Liu, J. B., Johnson, H. T., Sehitoglu, H., and Johnson, D. D., 2009, "Quantitative prediction of twinning stress in fcc alloys: Application to Cu-Al," Physical Review B, 79(21), p. 214202.
[71] Ojha, A., Sehitoglu, H., Patriarca, L., and Maier, H., 2014, "Twin migration in Fe-based bcc crystals: theory and experiments," Philosophical Magazine, 94(16), pp. 1816-1840.
[72] Joos, B., Ren, Q., and Duesbery, M., 1994, "Peierls-Nabarro model of dislocations in silicon with generalized stacking-fault restoring forces," Physical Review B, 50(9), p. 5890.
[73] Schoeck, G., 1994, "The generalized Peierls–Nabarro model," Philosophical Magazine A, 69(6), pp. 1085-1095.
[74] Peierls, R., 1940, "The size of a dislocation," Proceedings of the Physical Society, 52(1), pp. 34-37.
[75] Nabarro, F., 1947, "Dislocations in a simple cubic lattice," Proceedings of the Physical Society, 59(2), p. 256.
[76] Kibey, S., Liu, J., Johnson, D., and Sehitoglu, H., 2007, "Predicting twinning stress in fcc metals: Linking twin-energy pathways to twin nucleation," Acta Materialia, 55(20), pp. 6843-6851.
[77] Koning, M. d., Miller, R., Bulatov, V., and Abraham, F. F., 2002, "Modelling grain-boundary resistance in intergranular dislocation slip transmission," Philosophical Magazine A, 82(13), pp. 2511-2527.
[78] Hirth, J. P., and Lothe, J., 1982, "Theory of dislocations."
[79] Mahajan, S., and Chin, G., 1974, "The interaction of twins with existing substructure and twins in cobalt-iron alloys," Acta Metallurgica, 22(9), pp. 1113-1119.
[80] Li, J., 1960, "The interaction of parallel edge dislocations with a simple tilt dislocation wall," Acta Metallurgica, 8(5), pp. 296-311.
[81] Li, J., and Chalmers, B., 1963, "Energy of a wall of extended dislocations," Acta Metallurgica, 11(4), pp. 243-249.
[82] Li, J. C., and Needham, C. D., 1960, "Some elastic properties of a screw dislocation wall," Journal of Applied Physics, 31(8), pp. 1318-1330.
[83] Neumann, P., 1986, "Low energy dislocation configurations: a possible key to the understanding of fatigue," Materials Science and Engineering, 81, pp. 465-475.
[84] Lu, L., Chen, X., Huang, X., and Lu, K., 2009, "Revealing the maximum strength in nanotwinned copper," Science, 323(5914), pp. 607-610.
[85] Lu, L., Shen, Y., Chen, X., Qian, L., and Lu, K., 2004, "Ultrahigh strength and high electrical conductivity in copper," Science, 304(5669), pp. 422-426.
[86] Deng, C., and Sansoz, F., 2009, "Fundamental differences in the plasticity of periodically twinned nanowires in Au, Ag, Al, Cu, Pb and Ni," Acta Materialia, 57(20), pp. 6090-6101.
[87] Asaro, R. J., and Suresh, S., 2005, "Mechanistic models for the activation volume and rate sensitivity in metals with nanocrystalline grains and nano-scale twins," Acta Materialia, 53(12), pp. 3369-3382.
[88] Lu, L., Schwaiger, R., Shan, Z., Dao, M., Lu, K., and Suresh, S., 2005, "Nano-sized twins induce high rate sensitivity of flow stress in pure copper," Acta Materialia, 53(7), pp. 2169-2179.
[89] Wei, Q., Cheng, S., Ramesh, K., and Ma, E., 2004, "Effect of nanocrystalline and ultrafine grain sizes on the strain rate sensitivity and activation volume: fcc versus bcc metals," Materials Science and Engineering: A, 381(1), pp. 71-79.
[90] Jennings, A. T., Li, J., and Greer, J. R., 2011, "Emergence of strain-rate sensitivity in Cu nanopillars: Transition from dislocation multiplication to dislocation nucleation," Acta Materialia, 59(14), pp. 5627-5637.
[91] Lim, L., 1984, "Slip-twin interactions in nickel at 573K at large strains," Scripta metallurgica, 18(10), pp. 1139-1142.
[92] Evans, J., 1974, "Heterogeneous shear of a twin boundary in α-brass," scripta METALLURGICA, 8(9), pp. 1099-1103.

[93] Deng, C., and Sansoz, F., 2009, "Size-dependent yield stress in twinned gold nanowires mediated by site-specific surface dislocation emission," Applied Physics Letters, 95(9), p. 091914.
[94] Ezaz, T., Sangid, M. D., and Sehitoglu, H., 2011, "Energy barriers associated with slip–twin interactions," Philosophical Magazine, 91(10), pp. 1464-1488.
[95] Wu, Z., Zhang, Y., and Srolovitz, D., 2009, "Dislocation–twin interaction mechanisms for ultrahigh strength and ductility in nanotwinned metals," Acta Materialia, 57(15), pp. 4508-4518.
[96] Hartley, C. S., and Blachon, D. L., 1978, "Reactions of slip dislocations at coherent twin boundaries in face- centered- cubic metals," Journal of Applied Physics, 49(9), pp. 4788-4796.
[97] Lee, T., Robertson, I., and Birnbaum, H., 1990, "AnIn Situ transmission electron microscope deformation study of the slip transfer mechanisms in metals," Metallurgical Transactions A, 21(9), pp. 2437-2447.
[98] Kulkarni, Y., and Asaro, R. J., 2009, "Are some nanotwinned fcc metals optimal for strength, ductility and grain stability?," Acta Materialia, 57(16), pp. 4835-4844.
[99] Müllner, P., and Solenthaler, C., 1997, "On the effect of deformation twinning on defect densities," Materials Science and Engineering: A, 230(1), pp. 107-115.
[100] El Kadiri, H., and Oppedal, A., 2010, "A crystal plasticity theory for latent hardening by glide twinning through dislocation transmutation and twin accommodation effects," Journal of the Mechanics and Physics of Solids, 58(4), pp. 613-624.
[101] Jin, Z.-H., Gumbsch, P., Albe, K., Ma, E., Lu, K., Gleiter, H., and Hahn, H., 2008, "Interactions between non-screw lattice dislocations and coherent twin boundaries in face-centered cubic metals," Acta Materialia, 56(5), pp. 1126-1135.
[102] Mahajan, S., and Chin, G., 1973, "Twin-slip, twin-twin and slip-twin interactions in Co-8 wt.% Fe alloy single crystals," Acta Metallurgica, 21(2), pp. 173-179.
[103] Alkan, S., Chowdhury, P., Sehitoglu, H., Rateick, R. G., and Maier, H. J., 2016, "Role of nanotwins on fatigue crack growth resistance–Experiments and theory," International Journal of Fatigue, 84, pp. 28-39.
[104] Chowdhury, P. B., Sehitoglu, H., Rateick, R. G., and Maier, H. J., 2013, "Modeling fatigue crack growth resistance of nanocrystalline alloys," Acta Materialia, 61(7), pp. 2531-2547.
[105] Chowdhury, P., Sehitoglu, H., and Rateick, R., 2016, "Recent advances in modeling fatigue cracks at microscale in the presence of high density coherent twin interfaces," Current Opinion in Solid State and Materials Science, 20(3), pp. 140-150.
[106] Zhang, R., Wang, J., Beyerlein, I., and Germann, T., 2011, "Twinning in bcc metals under shock loading: a challenge to empirical potentials," Philosophical Magazine Letters, 91(12), pp. 731-740.
[107] Shi, Z., and Singh, C. V., 2016, "Competing twinning mechanisms in body-centered cubic metallic nanowires," Scripta Materialia, 113, pp. 214-217.
[108] Estrin, Y., and Mecking, H., 1984, "A unified phenomenological description of work hardening and creep based on one-parameter models," Acta Metallurgica, 32(1), pp. 57-70.
[109] Jackson, P., and Basinski, Z., 1967, "Latent hardening and the flow stress in copper single crystals," Canadian Journal of Physics, 45(2), pp. 707-735.
[110] Friedel, J., 1955, "CXXX. On the linear work hardening mate of face-centred cubic single crystals," Philosophical Magazine, 46(382), pp. 1169-1186.
[111] Lomer, W., 1951, "A dislocation reaction in the face-centred cubic lattice," Philosophical Magazine Series 7, 42(334), pp. 1327-1331.
[112] Garstone, J., and Honeycombe, R., 1957, "Dislocations and Mechanical Properties of Crystals," J. Wiley, New York, p. 391.
[113] Robertson, I. M., 1986, "Microtwin formation in deformed nickel," Philosophical Magazine A: Physics of Condensed Matter, Structure, Defects and Mechanical Properties, 54(6), pp. 821-835.
[114] Chowdhury, P., Canadinc, D., and Sehitoglu, H., 2017, "On deformation behavior of Fe-Mn based structural alloys," Materials Science and Engineering: R: Reports, 122, pp. 1-28.
[115] Yamakov, V., Wolf, D., Phillpot, S. R., Mukherjee, A. K., and Gleiter, H., 2002, "Dislocation processes in the deformation of nanocrystalline aluminium by molecular-dynamics simulation," Nature materials, 1(1), pp. 45-49.
[116] Shabib, I., and Miller, R. E., 2009, "Deformation characteristics and stress–strain response of nanotwinned copper via molecular dynamics simulation," Acta Materialia, 57(15), pp. 4364-4373.
[117] Li, X., Wei, Y., Lu, L., Lu, K., and Gao, H., 2010, "Dislocation nucleation governed softening and maximum strength in nano-twinned metals," Nature, 464(7290), pp. 877-880.

[118] Zhu, T., and Gao, H., 2012, "Plastic deformation mechanism in nanotwinned metals: An insight from molecular dynamics and mechanistic modeling," Scripta Materialia, 66(11), pp. 843-848.
[119] Chowdhury, P. B., 2011, "Fatigue crack growth (FCG) modeling in the presence of nano-obstacles," University of Illinois at Urbana-Champaign.
[120] Chowdhury, P., Sehitoglu, H., and Rateick, R., 2017, "Damage tolerance of carbon-carbon composites in aerospace application," Carbon.
[121] Rice, J. R., 1992, "Dislocation nucleation from a crack tip: an analysis based on the Peierls concept," Journal of the Mechanics and Physics of Solids, 40(2), pp. 239-271.
[122] Rice, J. R., and Thomson, R., 1974, "Ductile versus brittle behaviour of crystals," Philosophical magazine, 29(1), pp. 73-97.
[123] deCelis, B., Argon, A. S., and Yip, S., 1983, "Molecular dynamics simulation of crack tip processes in alpha- iron and copper," Journal of applied physics, 54(9), pp. 4864-4878.
[124] Chowdhury, P. B., Sehitoglu, H., and Rateick, R. G., 2014, "Predicting fatigue resistance of nano-twinned materials: Part I–Role of cyclic slip irreversibility and Peierls stress," International Journal of Fatigue, 68, pp. 277-291.
[125] Chowdhury, P. B., Sehitoglu, H., and Rateick, R. G., 2014, "Predicting fatigue resistance of nano-twinned materials: Part II–Effective threshold stress intensity factor range," International Journal of Fatigue, 68, pp. 292-301.
[126] Xie, C., Fang, Q. H., Liu, X., Guo, P. C., Chen, J. K., Zhang, M. H., Liu, Y. W., Rolfe, B., and Li, L. X., 2016, "Theoretical study on the deformation twinning and cracking in coarse-grained magnesium alloys," International Journal of Plasticity.
[127] Otsuka, K., and Wayman, C. M., 1999, Shape memory materials, Cambridge university press.
[128] Chowdhury, P., Patriarca, L., Ren, G., and Sehitoglu, H., 2016, "Molecular dynamics modeling of NiTi superelasticity in presence of nanoprecipitates," International Journal of Plasticity, 81, pp. 152-167.
[129] Lai, W., and Liu, B., 2000, "Lattice stability of some Ni-Ti alloy phases versus their chemical composition and disordering," Journal of Physics: Condensed Matter, 12(5), p. L53.
[130] Chowdhury, P., and Sehitoglu, H., 2016, "Significance of slip propensity determination in shape memory alloys," Scripta Materialia.
[131] Chowdhury, P., and Sehitoglu, H., 2017, "Deformation physics of shape memory alloys–fundamentals at atomistic frontier," Progress in Materials Science, 88, pp. 49-88.
[132] Mirzaeifar, R., Gall, K., Zhu, T., Yavari, A., and DesRoches, R., 2014, "Structural transformations in NiTi shape memory alloy nanowires," Journal of Applied Physics, 115(19), p. 194307.
[133] Mutter, D., and Nielaba, P., 2013, "Simulation of the shape memory effect in a NiTi nano model system," Journal of Alloys and Compounds, 577, pp. S83-S87.
[134] Chowdhury, P., Ren, G., and Sehitoglu, H., 2015, "NiTi superelasticity via atomistic simulations," Philosophical Magazine Letters, pp. 1-13.
[135] Chowdhury, P., and Sehitoglu, H., 2016, "A revisit to atomistic rationale for slip in shape memory alloys," Progress in Materials Science.
[136] Wang, F., and Agnew, S. R., 2016, "Dislocation transmutation by tension twinning in magnesium alloy AZ31," International Journal of Plasticity, 81, pp. 63-86.
[137] El Kadiri, H., Baird, J. C., Kapil, J., Oppedal, A. L., Cherkaoui, M., and Vogel, S. C., 2013, "Flow asymmetry and nucleation stresses of twinning and non-basal slip in magnesium," International Journal of Plasticity, 44, pp. 111-120.
[138] Ishii, A., Li, J., and Ogata, S., 2016, "Shuffling-controlled versus strain-controlled deformation twinning: The case for HCP Mg twin nucleation," International Journal of Plasticity.
[139] Ngan, A., 1995, "A critique on some of the concepts regarding planar faults in crystals," Philosophical magazine letters, 72(1), pp. 11-19.
[140] Zimmerman, J. A., Gao, H., and Abraham, F. F., 2000, "Generalized stacking fault energies for embedded atom FCC metals," Modelling and Simulation in Materials Science and Engineering, 8(2), p. 103.
[141] Kibey, S., Liu, J. B., Johnson, D. D., and Sehitoglu, H., 2006, "Generalized planar fault energies and twinning in Cu–Al alloys," Applied physics letters, 89(19).
[142] Cai, W., and Bulatov, V. V., 2004, "Mobility laws in dislocation dynamics simulations," Materials Science and Engineering: A, 387, pp. 277-281.
[143] Devincre, B., Kubin, L., Lemarchand, C., and Madec, R., 2001, "Mesoscopic simulations of plastic deformation," Materials Science and Engineering: A, 309, pp. 211-219.

[144] Amodeo, R., and Ghoniem, N., 1990, "Dislocation dynamics. I. A proposed methodology for deformation micromechanics," Physical Review B, 41(10), p. 6958.
[145] Kocks, U. F., Argon, A. S., and Ashby, M. F., 1975, "Thermodynamics and Kinetics of Slip," Progress in Materials Science, 19.
[146] Clayton, J. D., 2010, Nonlinear mechanics of crystals, Springer Science & Business Media.

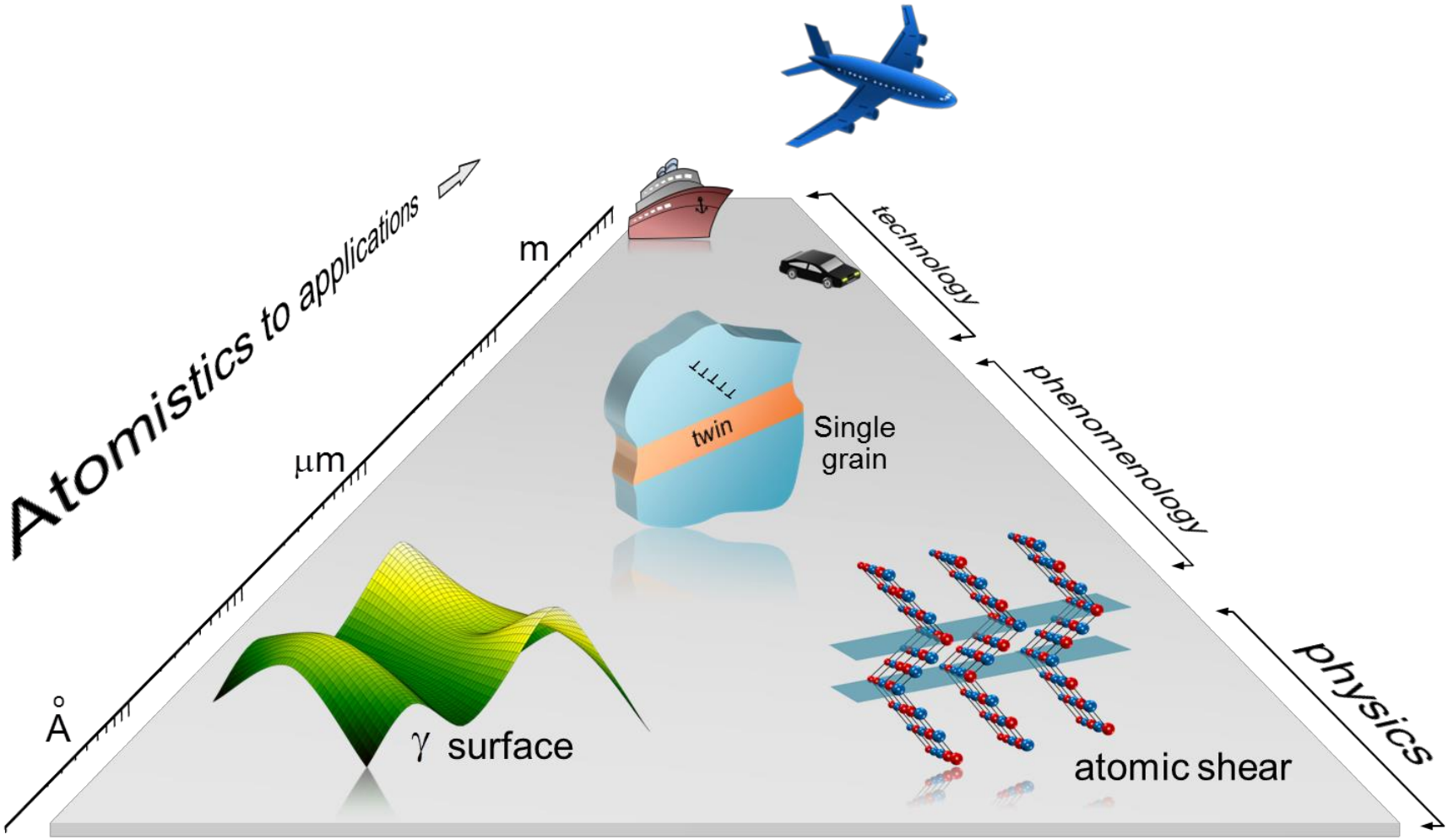
Atomistics to applications
m
μm
Å
technology
phenomenology
physics
twin
Single grain
γ surface
atomic shear

Figure 1

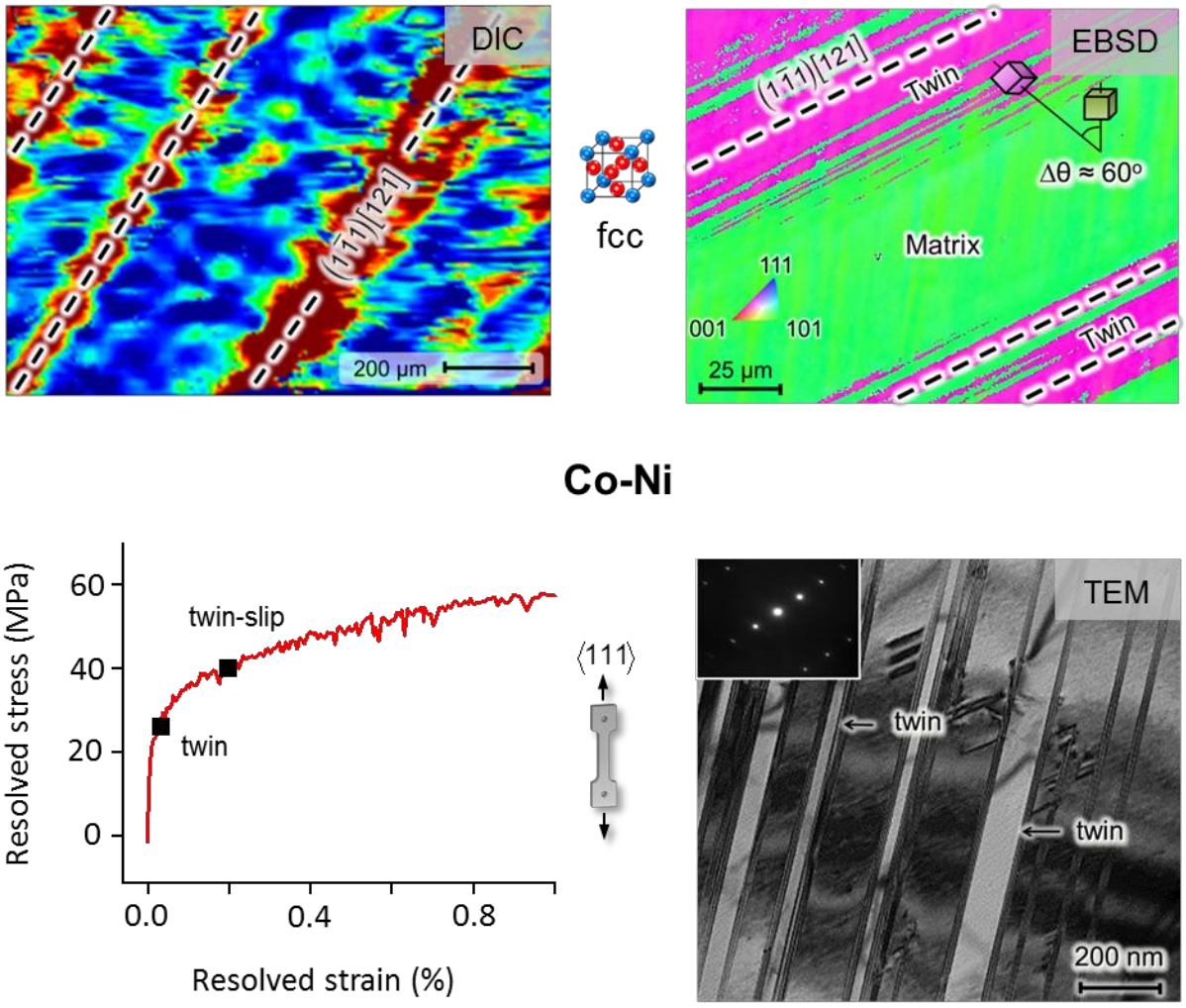
DIC
200 μm
fcc
EBSD
Twin
Δθ ≈ 60°
Matrix
111
001
101
25 μm
Twin
Co-Ni
Resolved stress (MPa)
60
40
20
0
twin-slip
twin
0.0
0.4
0.8
Resolved strain (%)
⟨111⟩
TEM
twin
twin
200 nm

Figure 2(a)

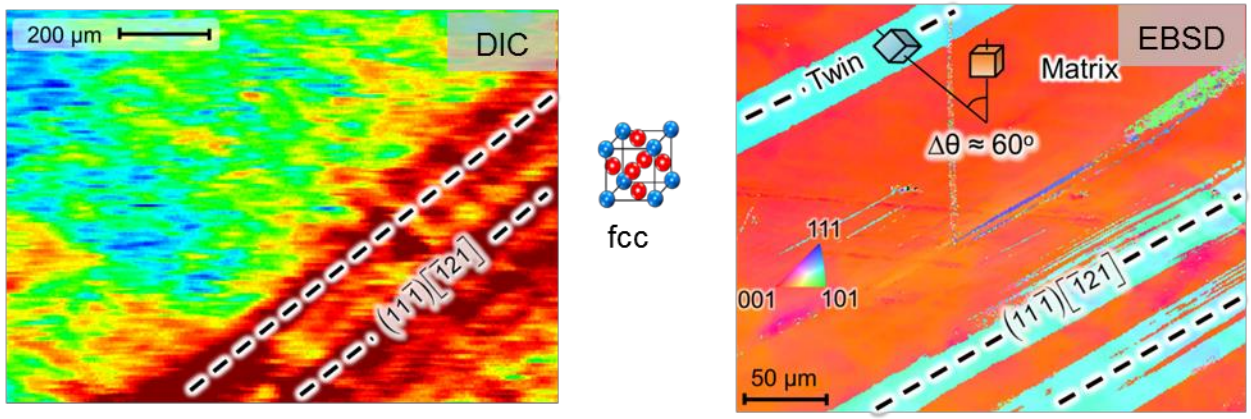

Co-Ni

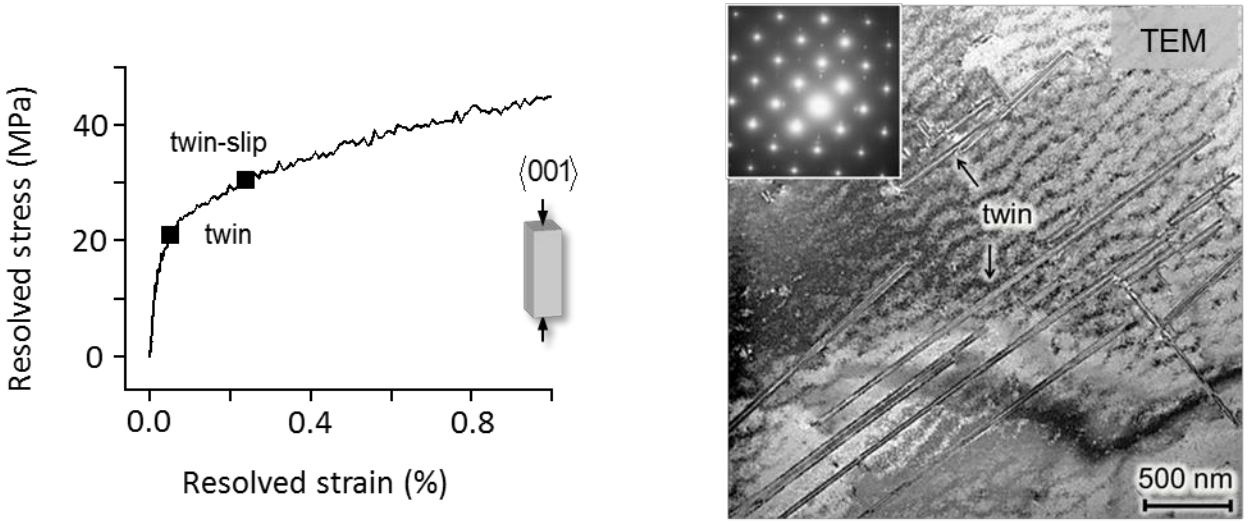

Figure 2(b)

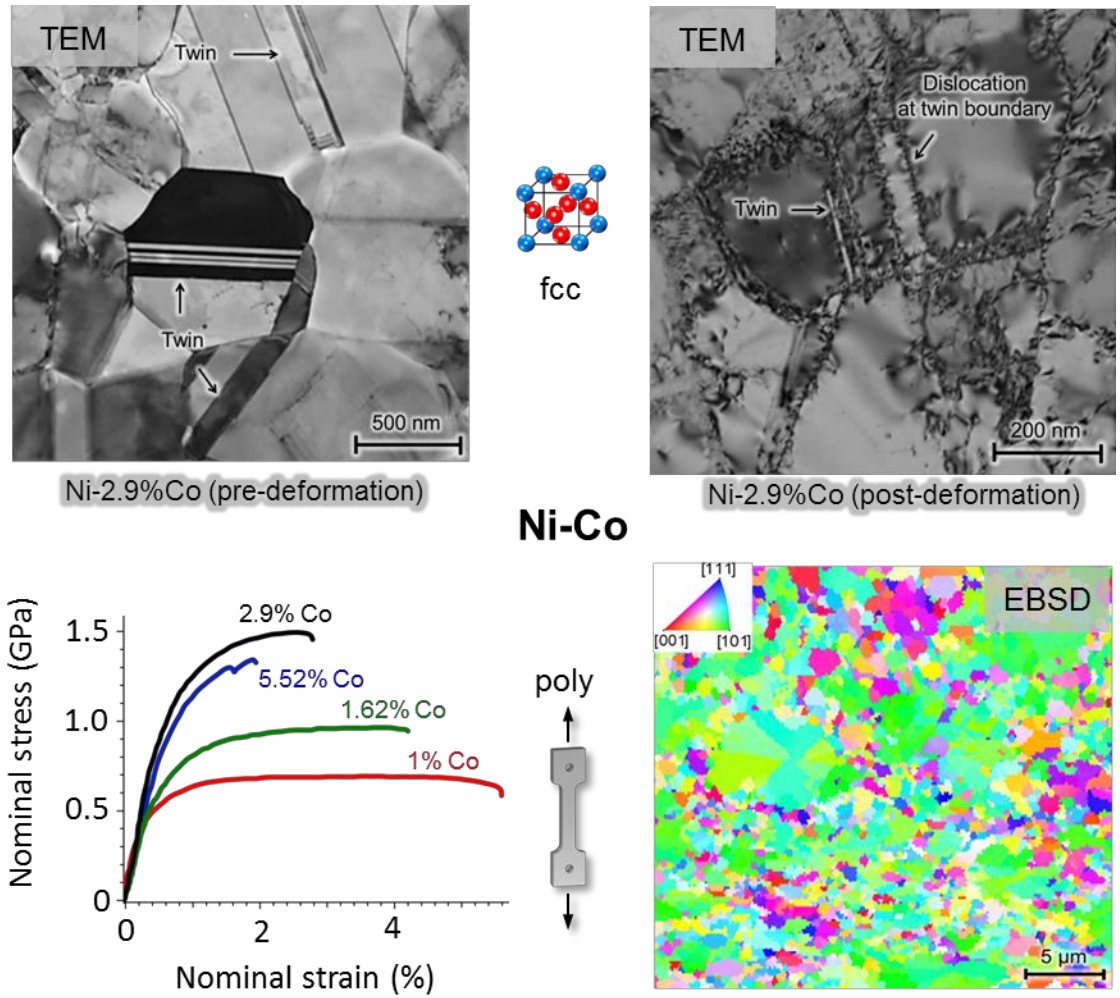
TEM
Twin
Twin
500 nm
Ni-2.9%Co (pre-deformation)
fcc
TEM
Dislocation
at twin boundary
Twin
200 nm
Ni-2.9%Co (post-deformation)
Ni-Co
Nominal stress (GPa)
1.5
1.0
0.5
0
0
2
4
Nominal strain (%)
2.9% Co
5.52% Co
1.62% Co
1% Co
poly
[111]
[001]
[101]
EBSD
5 μm

Figure 2(c)

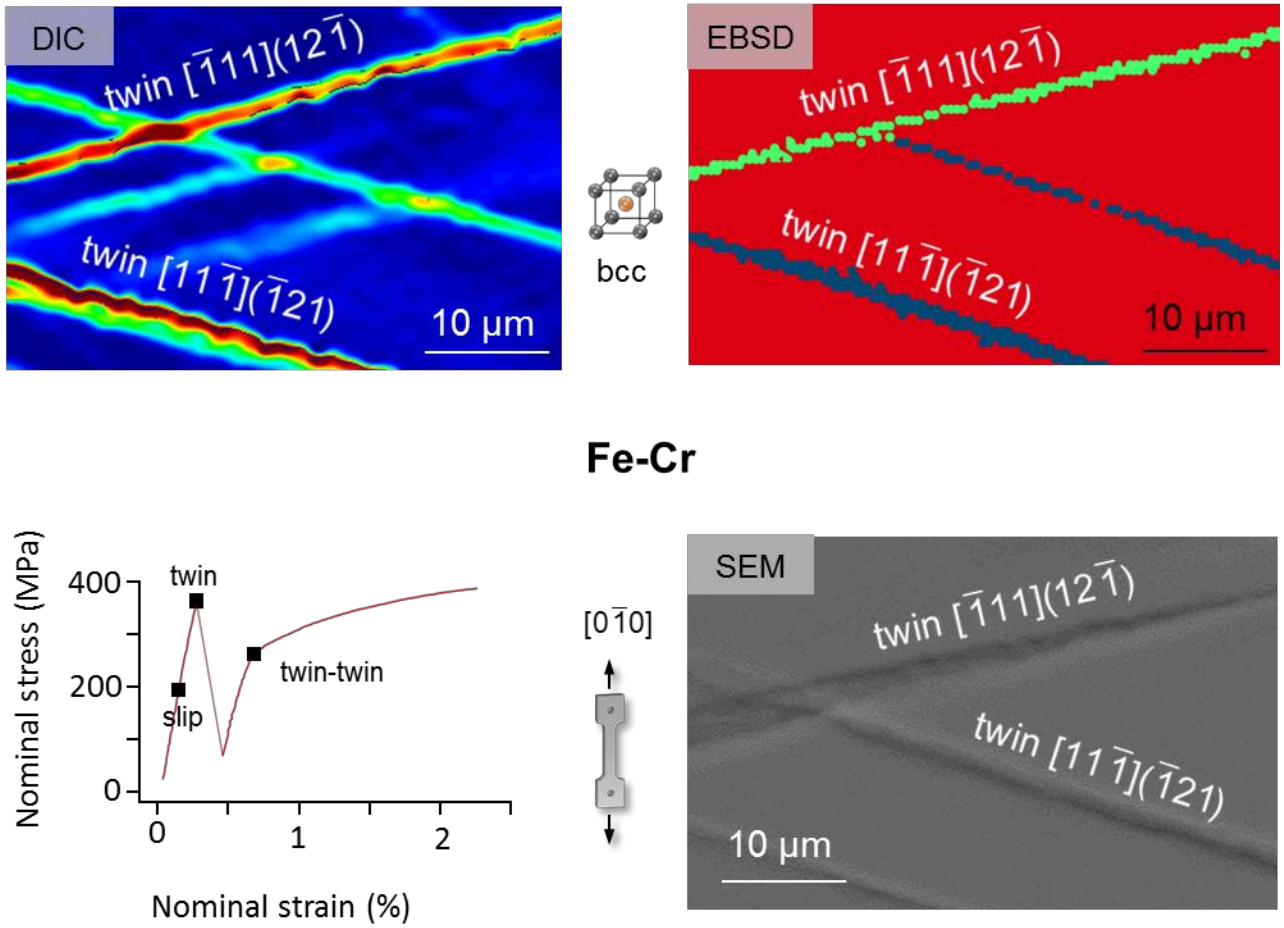
DIC
twin [$\bar{1}$11](12$\bar{1}$)
twin [11$\bar{1}$]($\bar{1}$21)
10 μm
bcc
EBSD
twin [$\bar{1}$11](12$\bar{1}$)
twin [11$\bar{1}$]($\bar{1}$21)
10 μm
Fe-Cr
Nominal stress (MPa)
400
200
0
twin
slip
twin-twin
0
1
2
Nominal strain (%)
[0$\bar{1}$0]
SEM
twin [$\bar{1}$11](12$\bar{1}$)
twin [11$\bar{1}$]($\bar{1}$21)
10 μm

Figure 3(a)

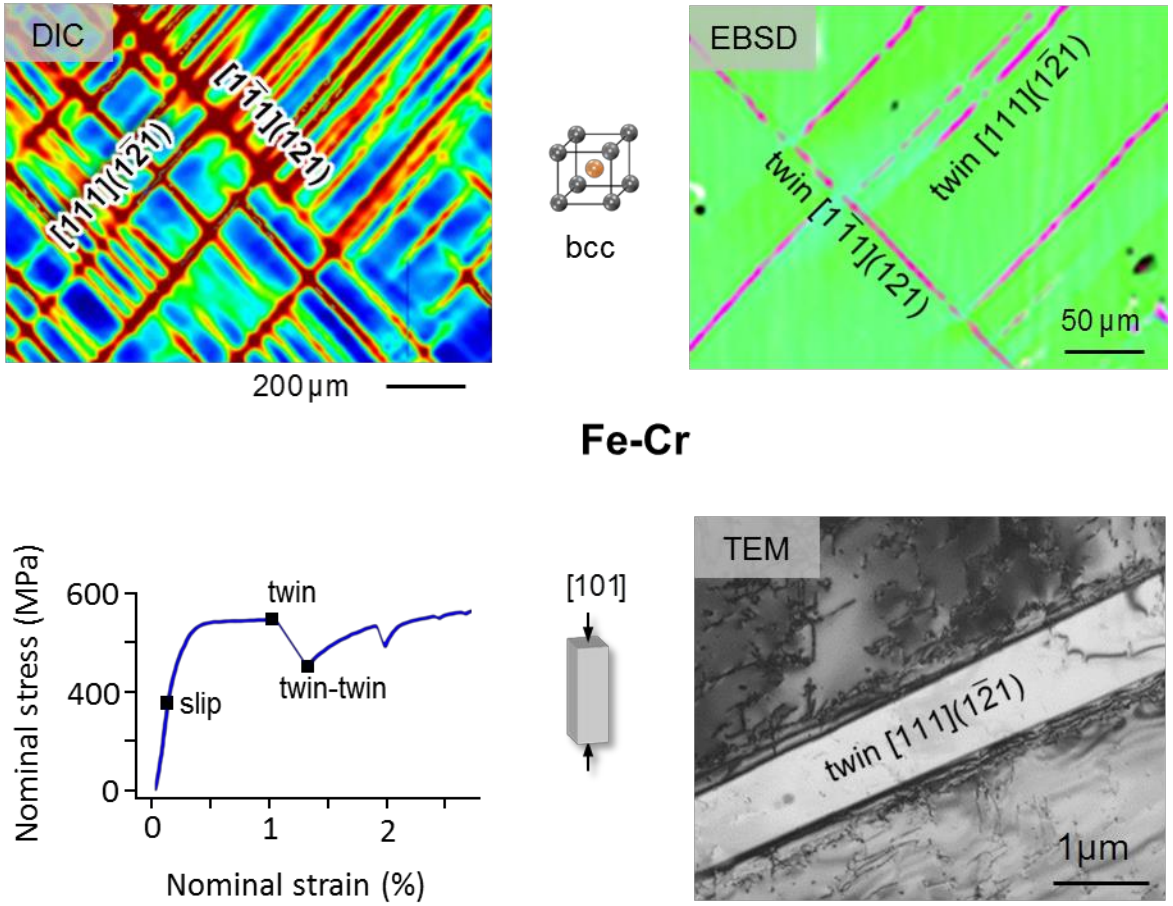
DIC
[1$\bar{1}$1](12$\bar{1}$)
[$\bar{1}$11](121)
200 µm
bcc
EBSD
twin [111](1$\bar{2}$1)
twin [1$\bar{1}$1](121)
50 µm
Fe-Cr
Nominal stress (MPa)
600
400
0
twin
slip
twin-twin
0
1
2
Nominal strain (%)
[101]
TEM
twin [111](1$\bar{2}$1)
1µm

Figure 3(b)

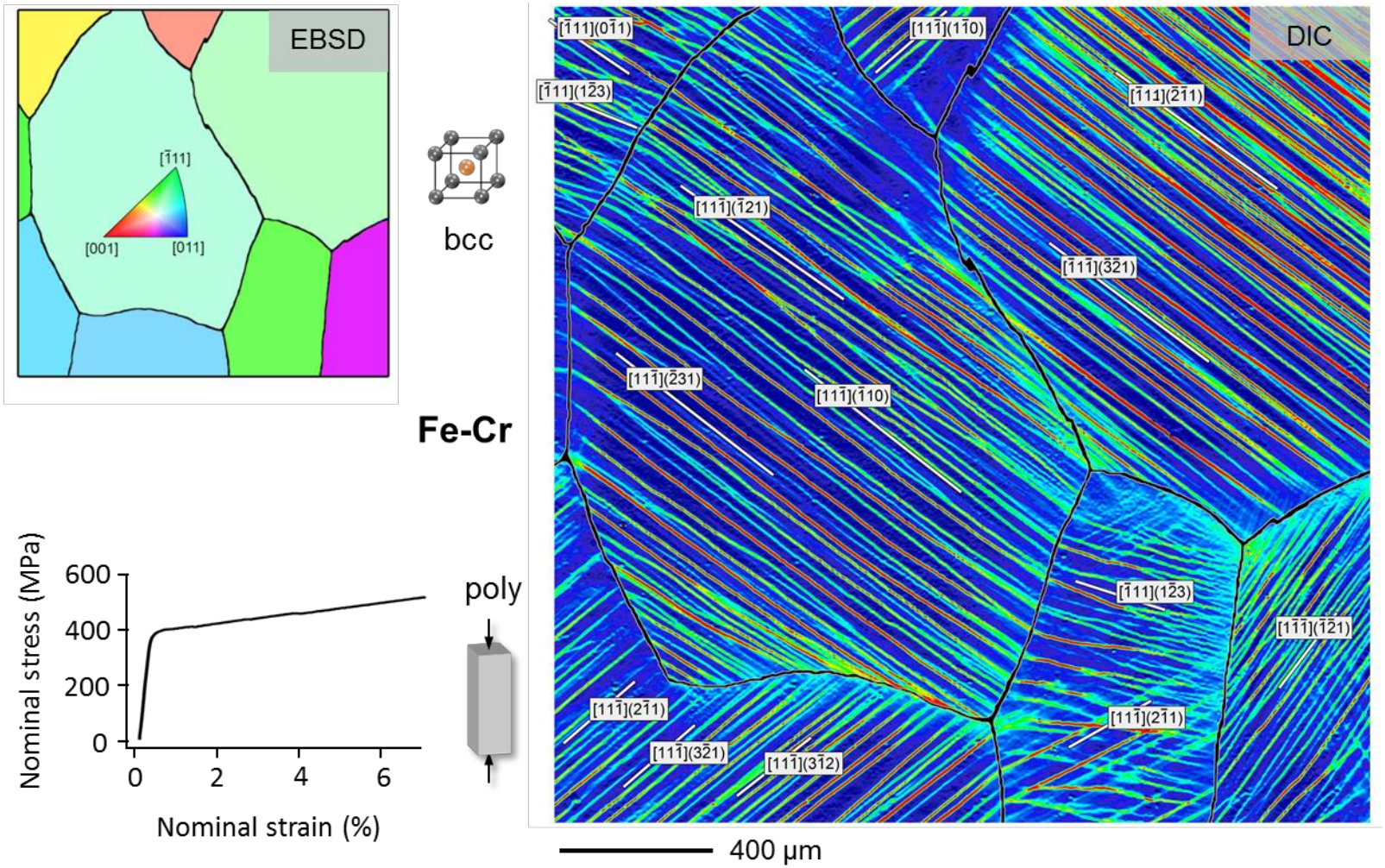
EBSD
[$\bar{1}$11]
[001]
[011]
bcc
Fe-Cr
poly
Nominal stress (MPa)
600
400
200
0
0
2
4
6
Nominal strain (%)
DIC
[$\bar{1}$11](0$\bar{1}$1)
[1$\bar{1}$1](1$\bar{1}$0)
[$\bar{1}$11](1$\bar{2}$3)
[$\bar{1}$11](2$\bar{1}$1)
[1$\bar{1}$1](1$\bar{2}$1)
[$\bar{1}$11](3$\bar{2}$1)
[11$\bar{1}$](2$\bar{3}$1)
[11$\bar{1}$](1$\bar{1}$0)
[$\bar{1}$11](1$\bar{2}$3)
[1$\bar{1}$1](1$\bar{2}$1)
[11$\bar{1}$](2$\bar{1}$1)
[11$\bar{1}$](2$\bar{1}$1)
[11$\bar{1}$](3$\bar{2}$1)
[11$\bar{1}$](3$\bar{1}$2)
400 µm

Figure 3(c)

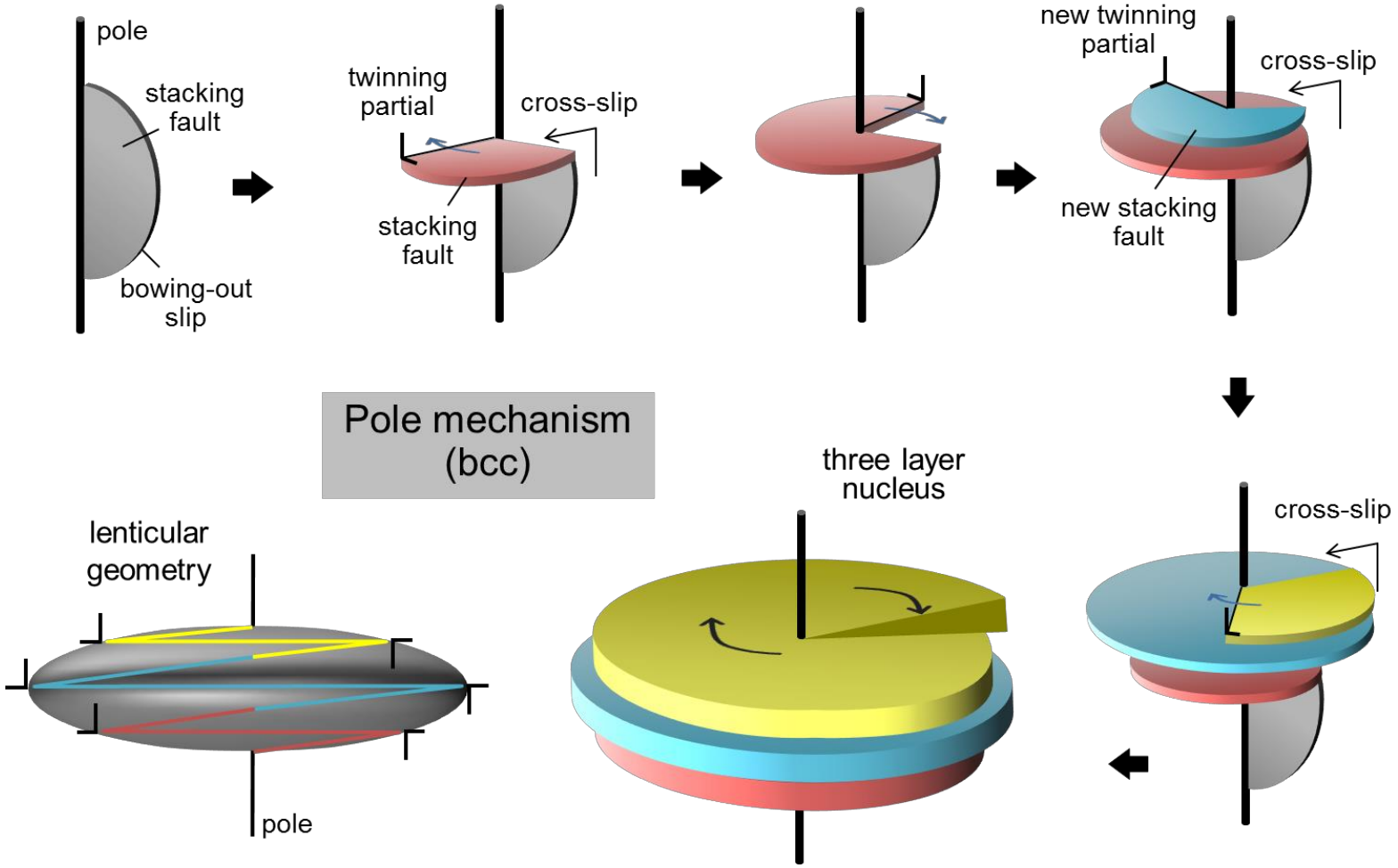
pole
stacking fault
bowing-out slip
twinning partial
cross-slip
stacking fault
new twinning partial
cross-slip
new stacking fault
Pole mechanism (bcc)
three layer nucleus
cross-slip
lenticular geometry
pole

Figure 4

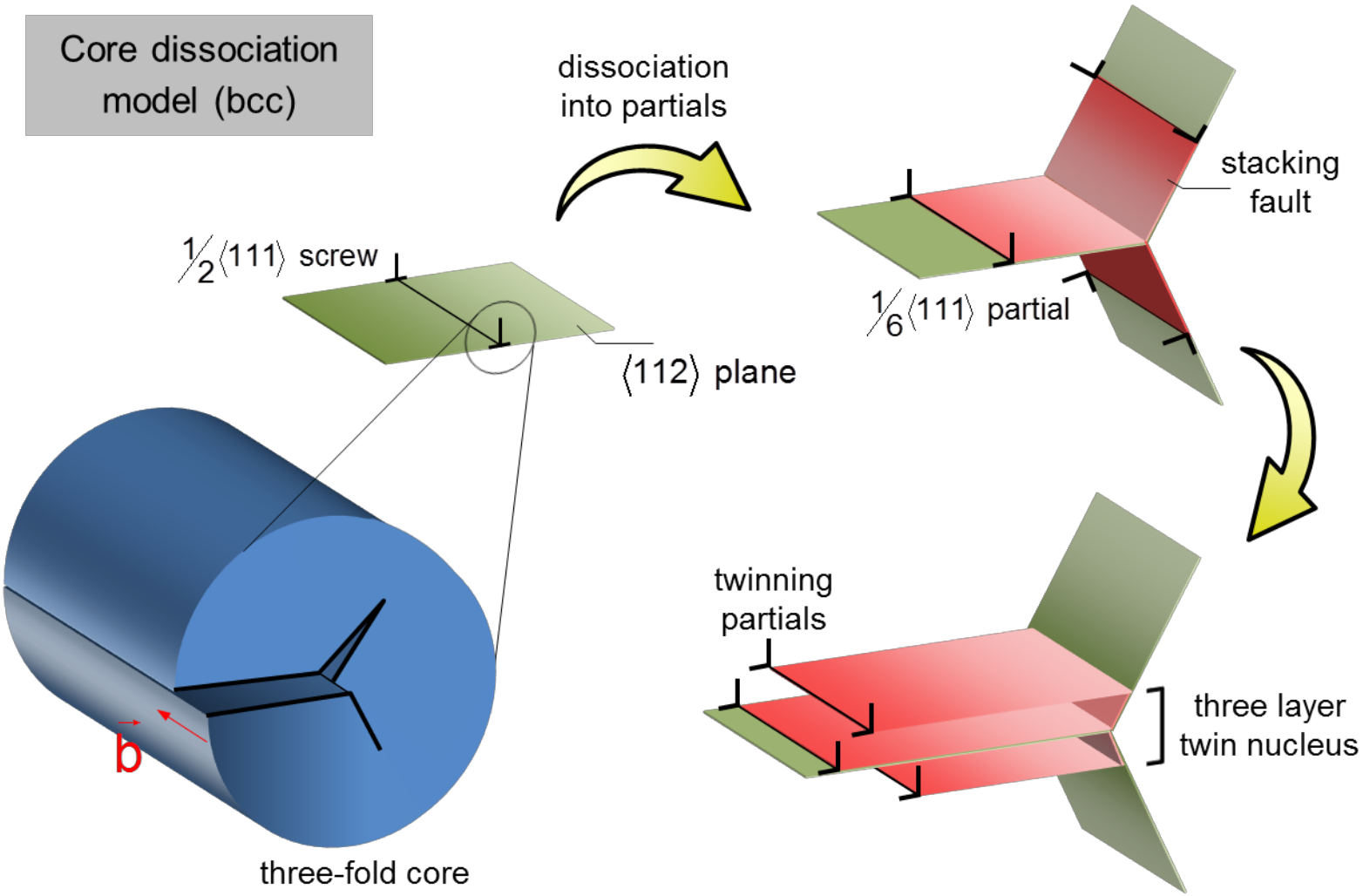
Core dissociation model (bcc)
dissociation into partials
stacking fault
$\frac{1}{2}\langle 111\rangle$ screw
$\frac{1}{6}\langle 111\rangle$ partial
$\langle 112\rangle$ plane
twinning partials
three layer twin nucleus
b
three-fold core

Figure 5

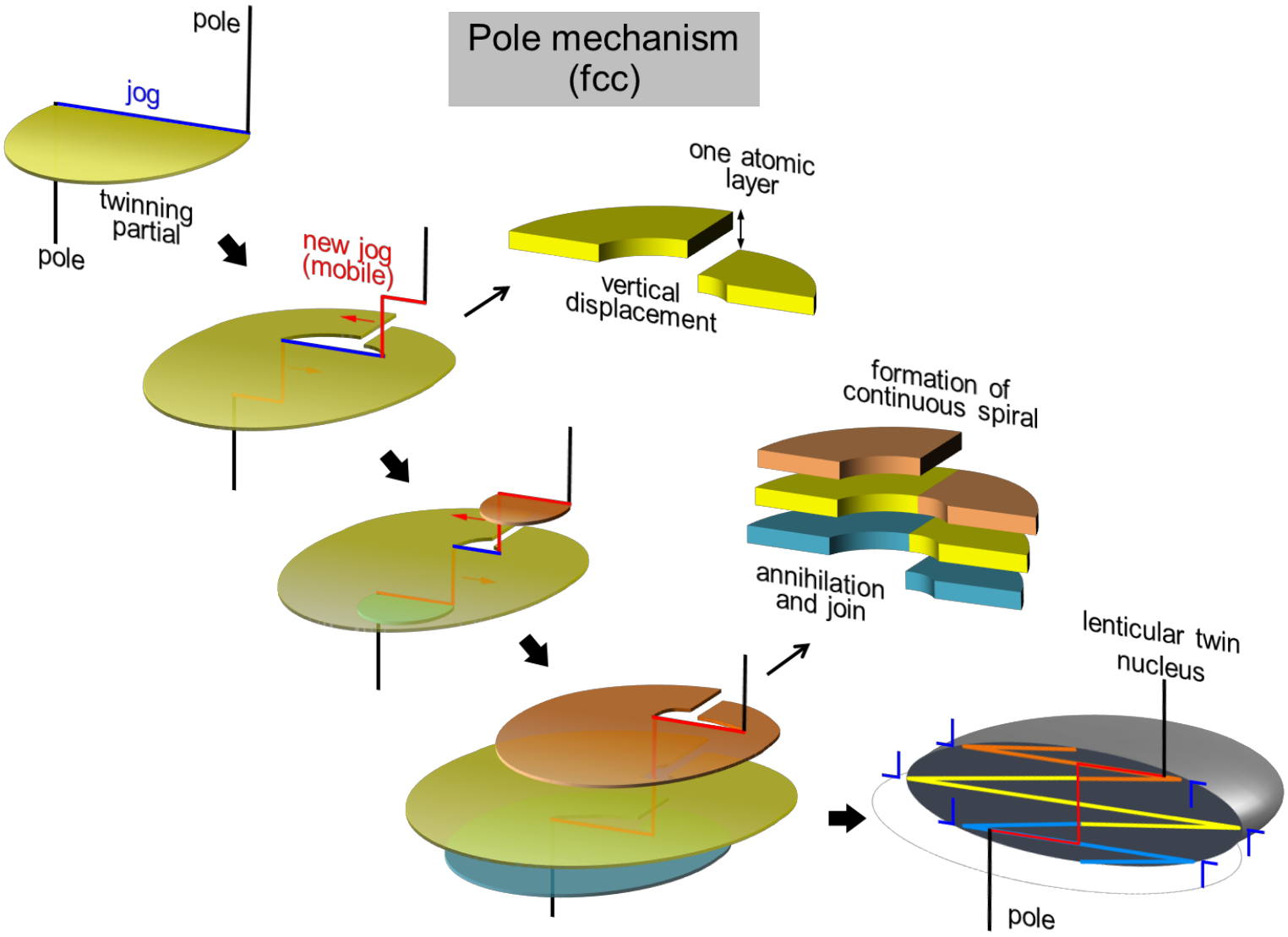
Pole mechanism
(fcc)
pole
jog
twinning
partial
pole
new jog
(mobile)
one atomic
layer
vertical
displacement
formation of
continuous spiral
annihilation
and join
lenticular twin
nucleus
pole

Figure 6

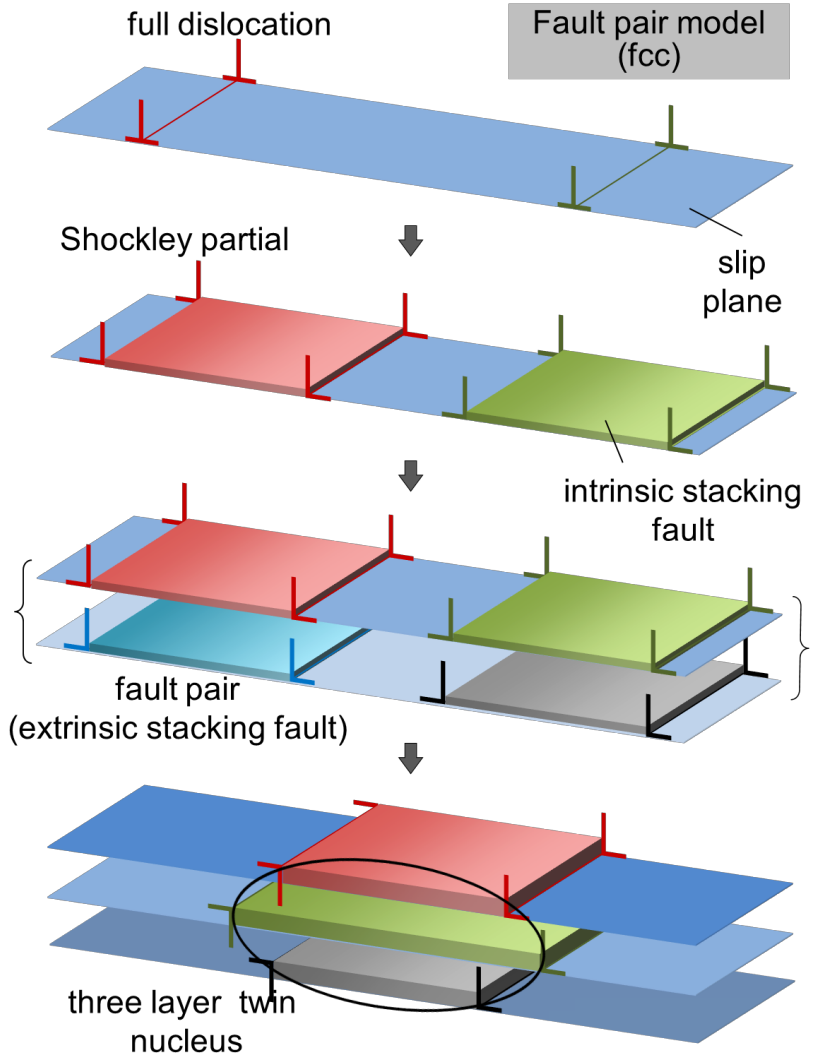
full dislocation
Fault pair model
(fcc)
Shockley partial
slip
plane
intrinsic stacking
fault
fault pair
(extrinsic stacking fault)
three layer twin
nucleus

Figure 7

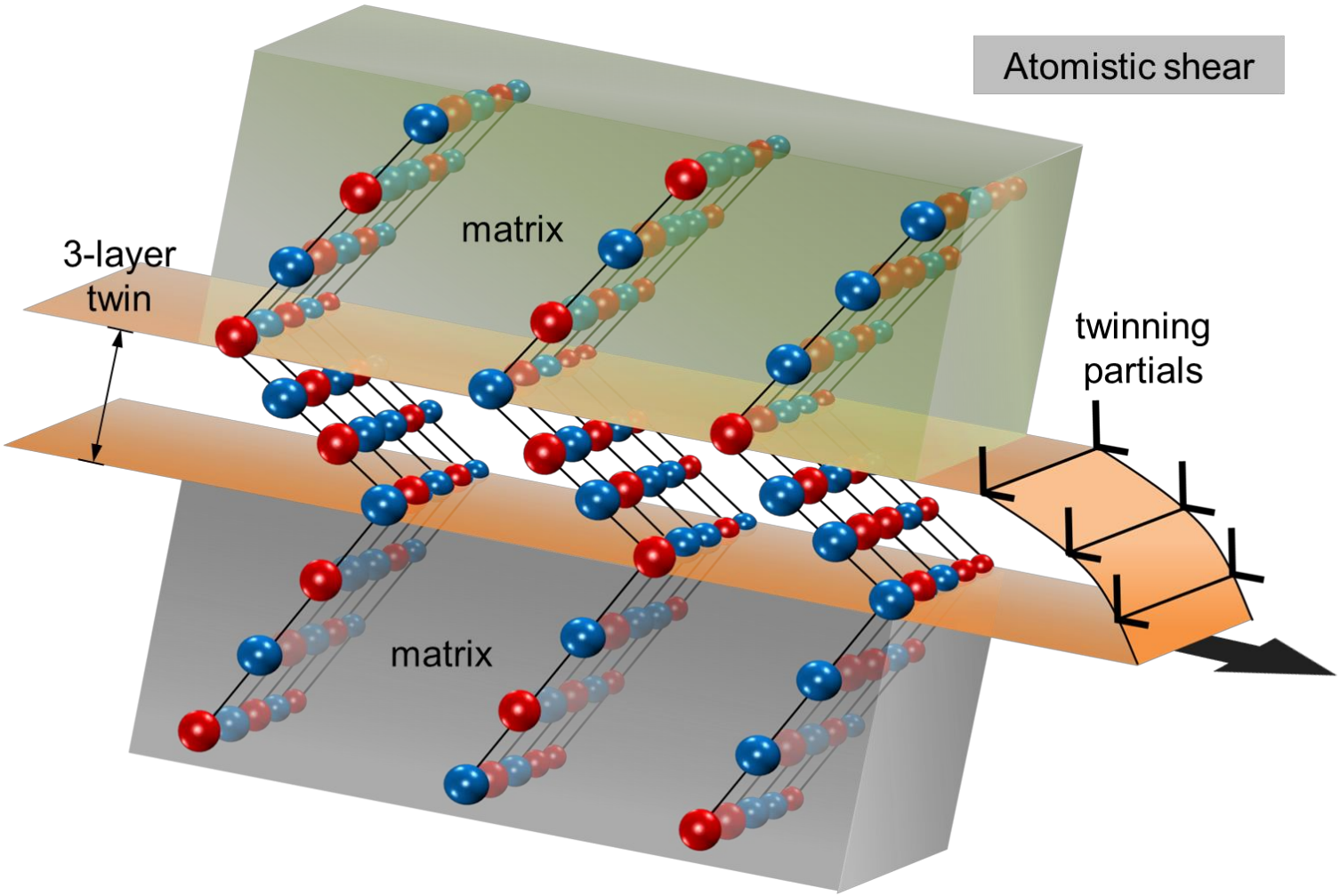
Atomistic shear
matrix
3-layer
twin
twinning
partials
matrix

Figure 8

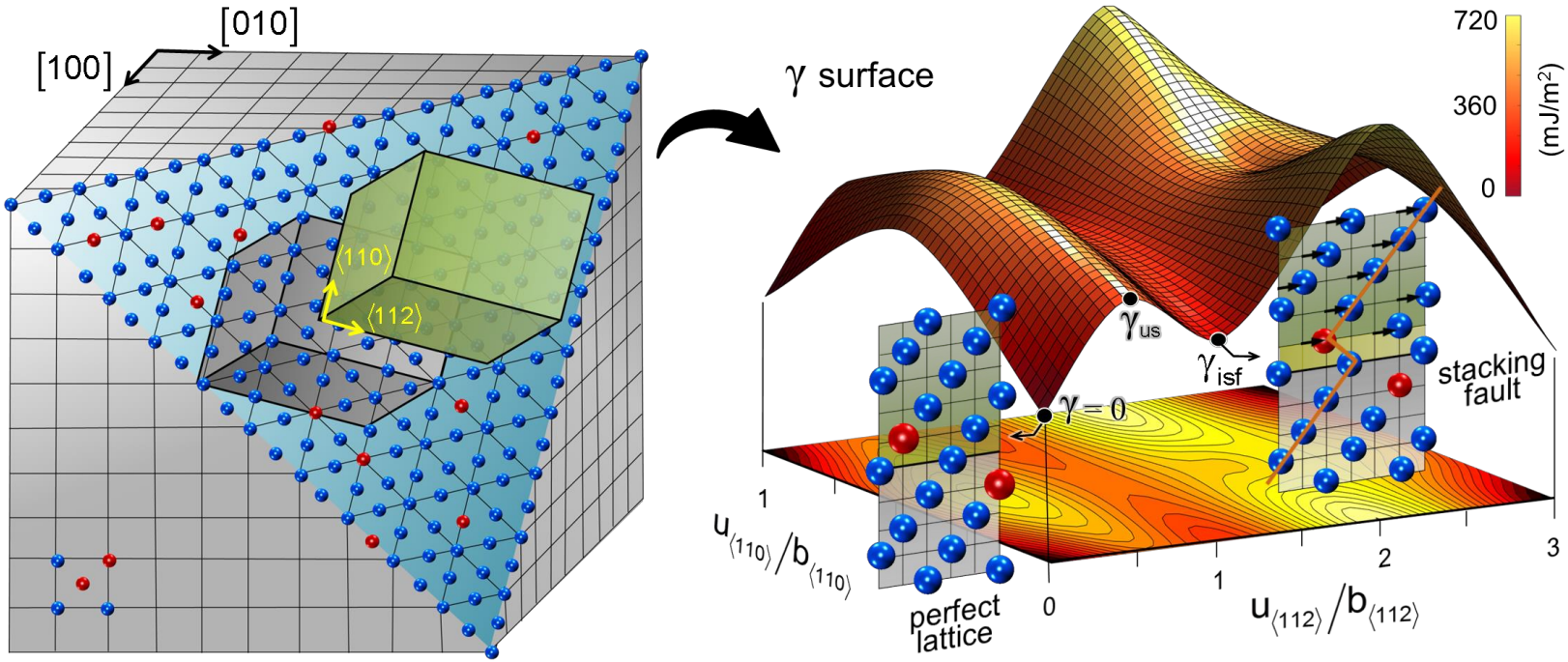
[010]
[100]
⟨110⟩
⟨112⟩
γ surface
720
360
0
(mJ/m²)
γus
γisf
γ = 0
stacking fault
perfect lattice
1
0
1
2
3
u⟨110⟩/b⟨110⟩
u⟨112⟩/b⟨112⟩

Figure 9

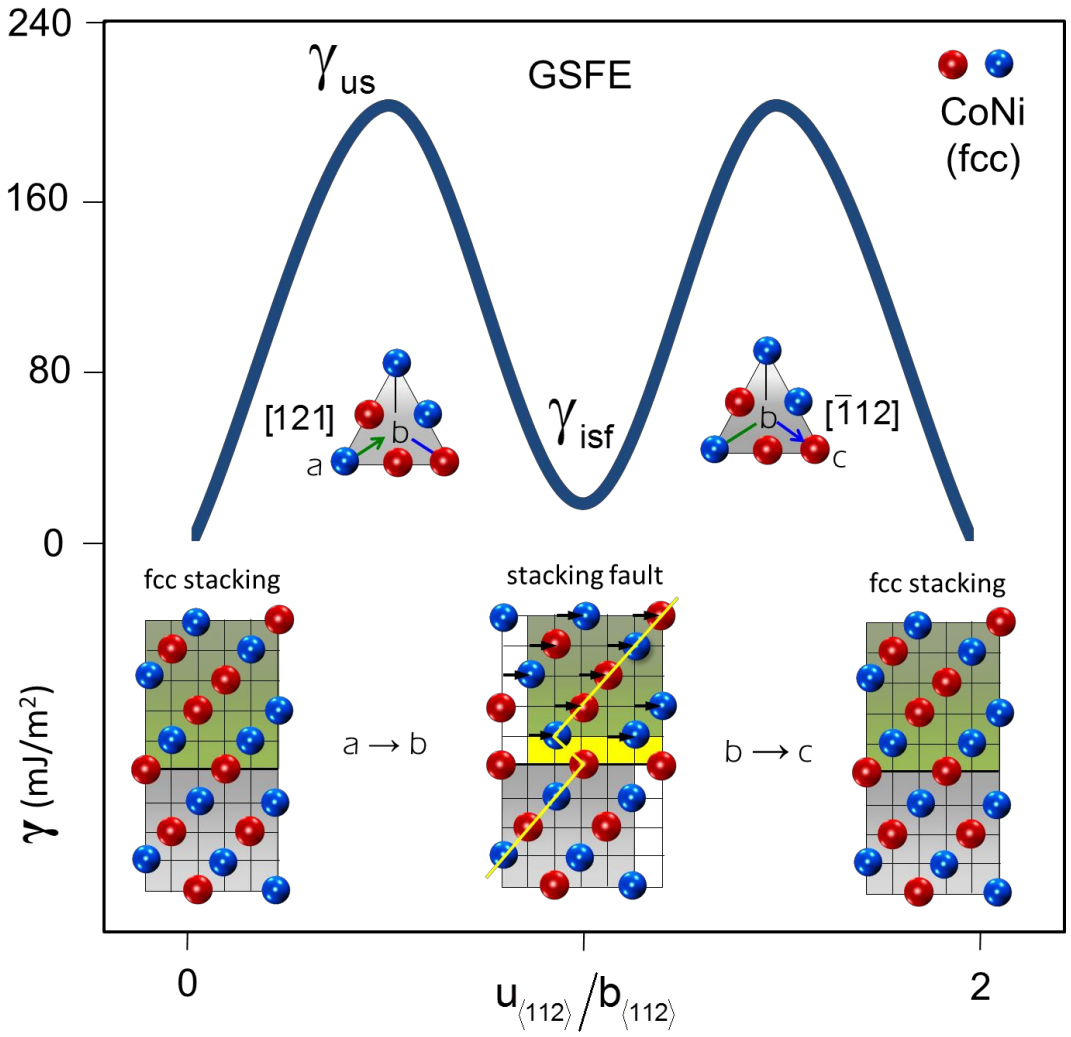
240
160
80
0
γ (mJ/m²)
γ us
GSFE
γ isf
CoNi
(fcc)
[121]
a
b
[$\bar{1}$12]
b
c
fcc stacking
stacking fault
fcc stacking
a → b
b → c
0
u⟨112⟩ /b⟨112⟩
2

Figure 10(a)

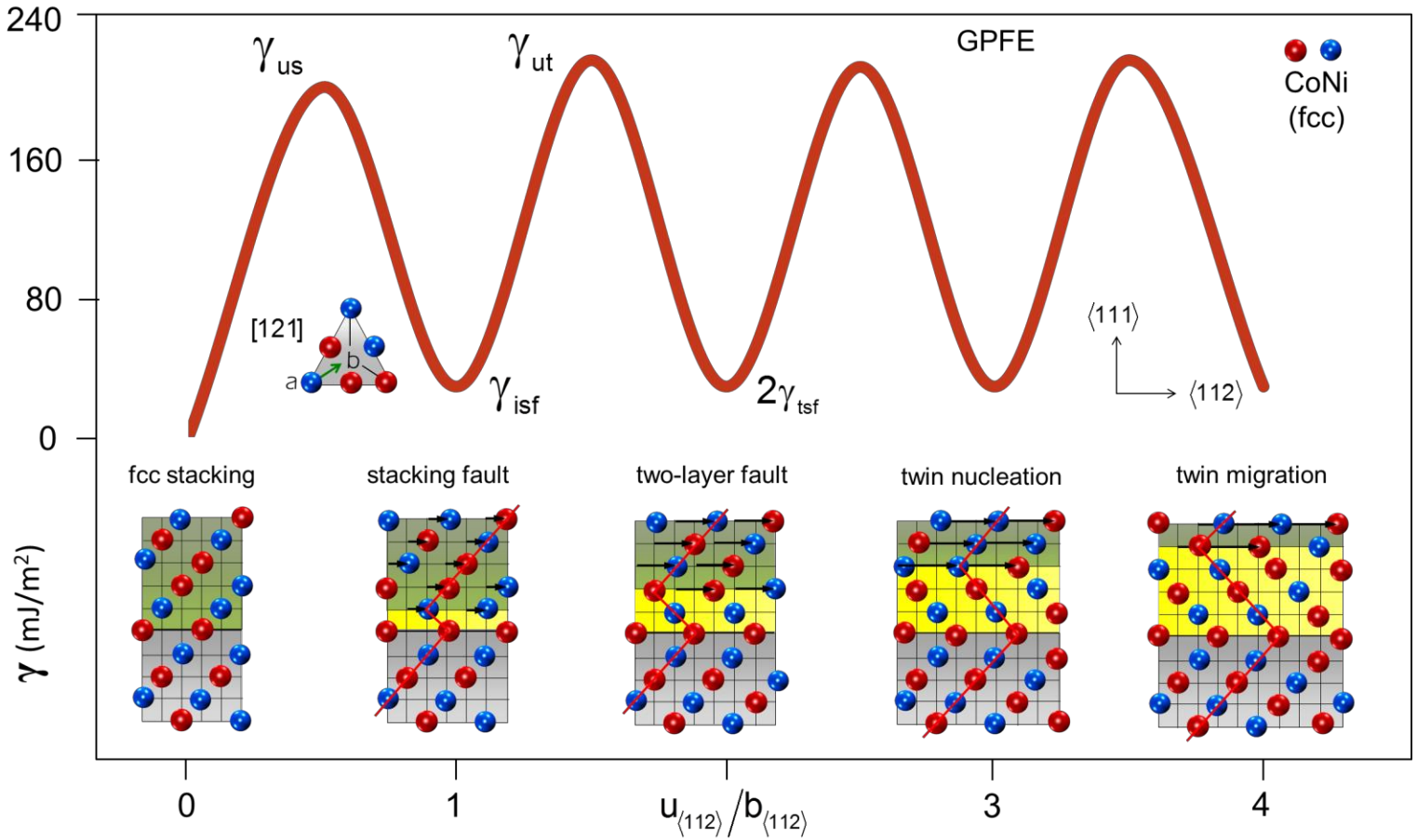
240
160
80
0
γ (mJ/m²)
γ us
γ ut
GPFE
CoNi
(fcc)
[121]
a
b
γ isf
2γ tsf
⟨111⟩
⟨112⟩
fcc stacking
stacking fault
two-layer fault
twin nucleation
twin migration
0
1
u⟨112⟩/b⟨112⟩
3
4

Figure 10(b)

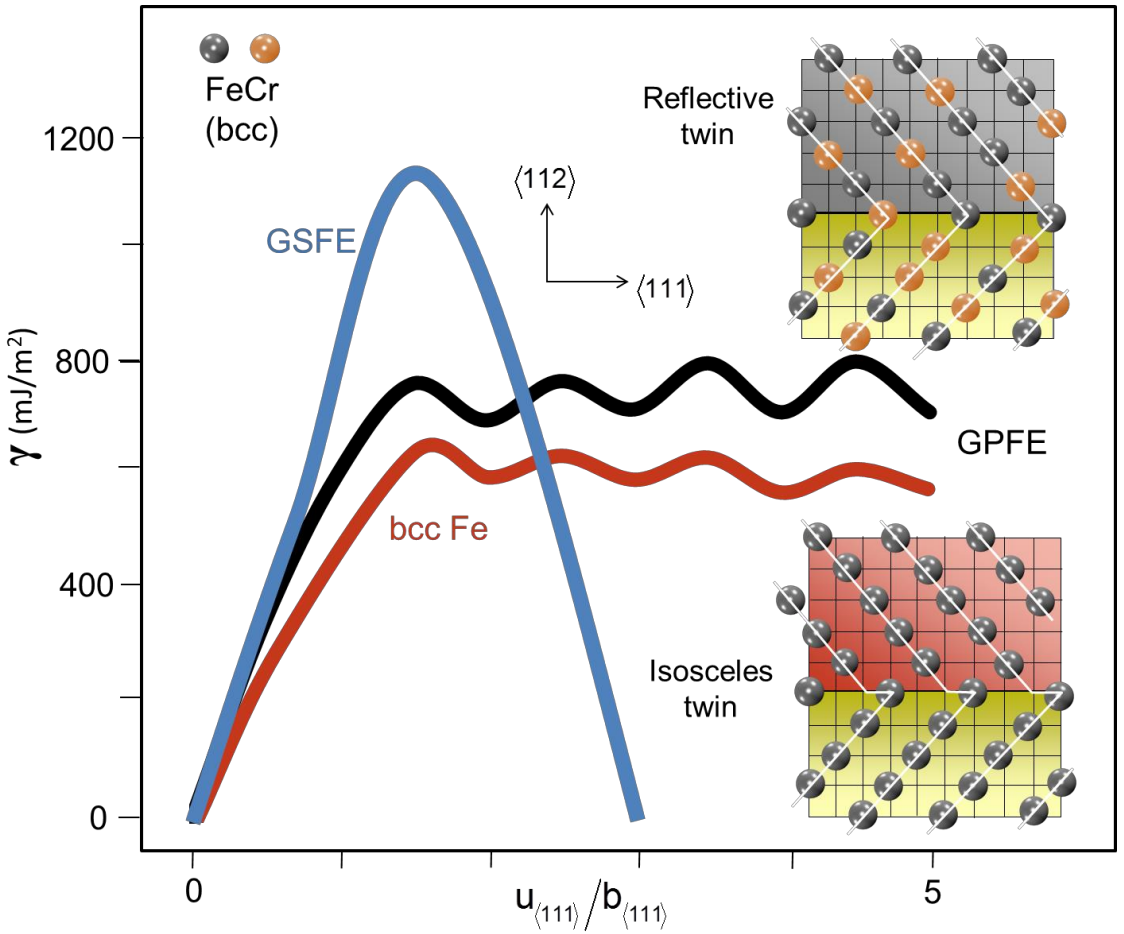
FeCr
(bcc)
Reflective
twin
⟨112⟩
⟨111⟩
GSFE
GPFE
bcc Fe
Isosceles
twin
1200
800
400
0
γ (mJ/m²)
0
5
u⟨111⟩/b⟨111⟩

Figure 10(c)

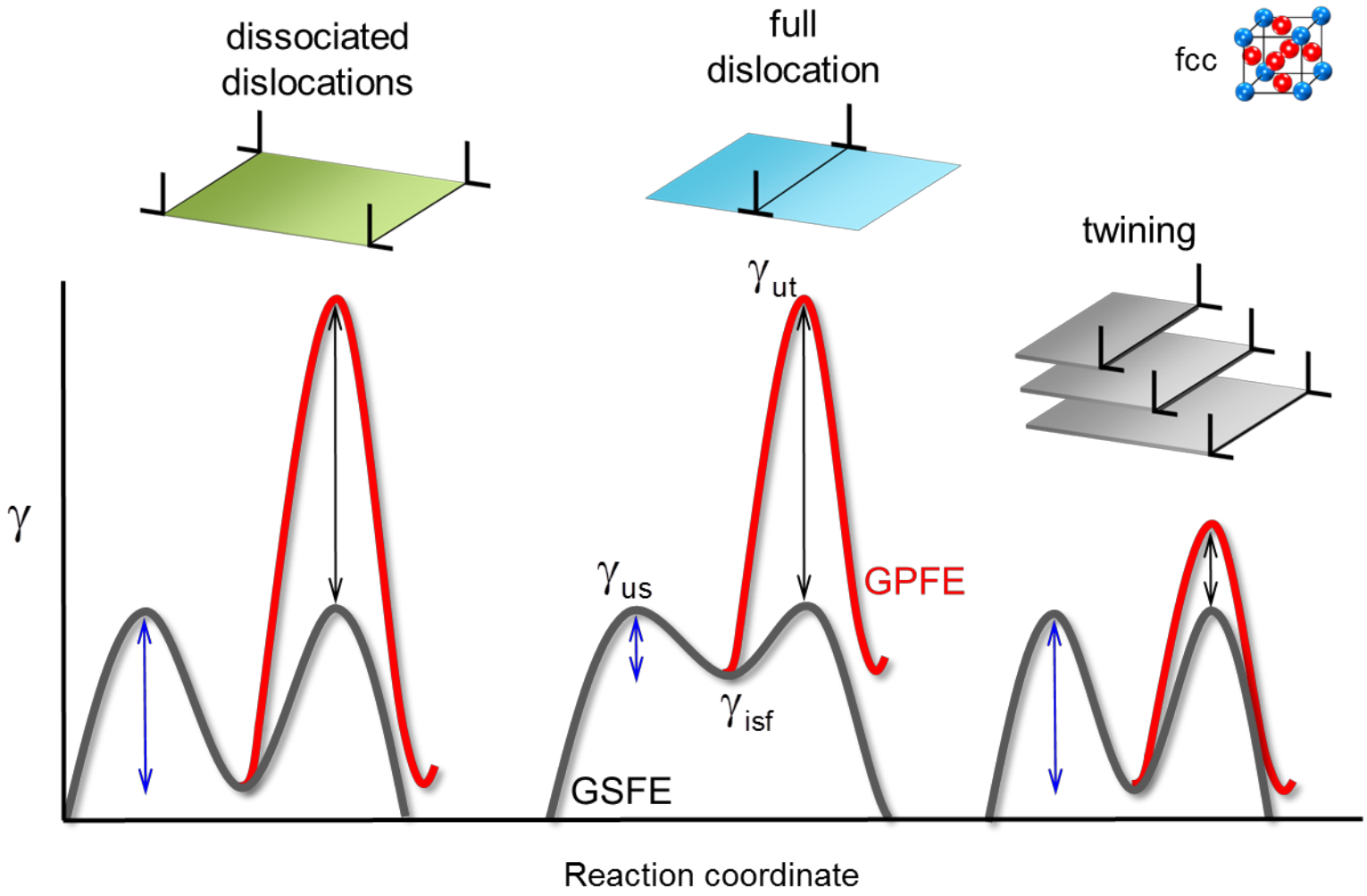
dissociated
dislocations
full
dislocation
fcc
twining
γ
γut
γus
γisf
GPFE
GSFE
Reaction coordinate

Figure 11(a)

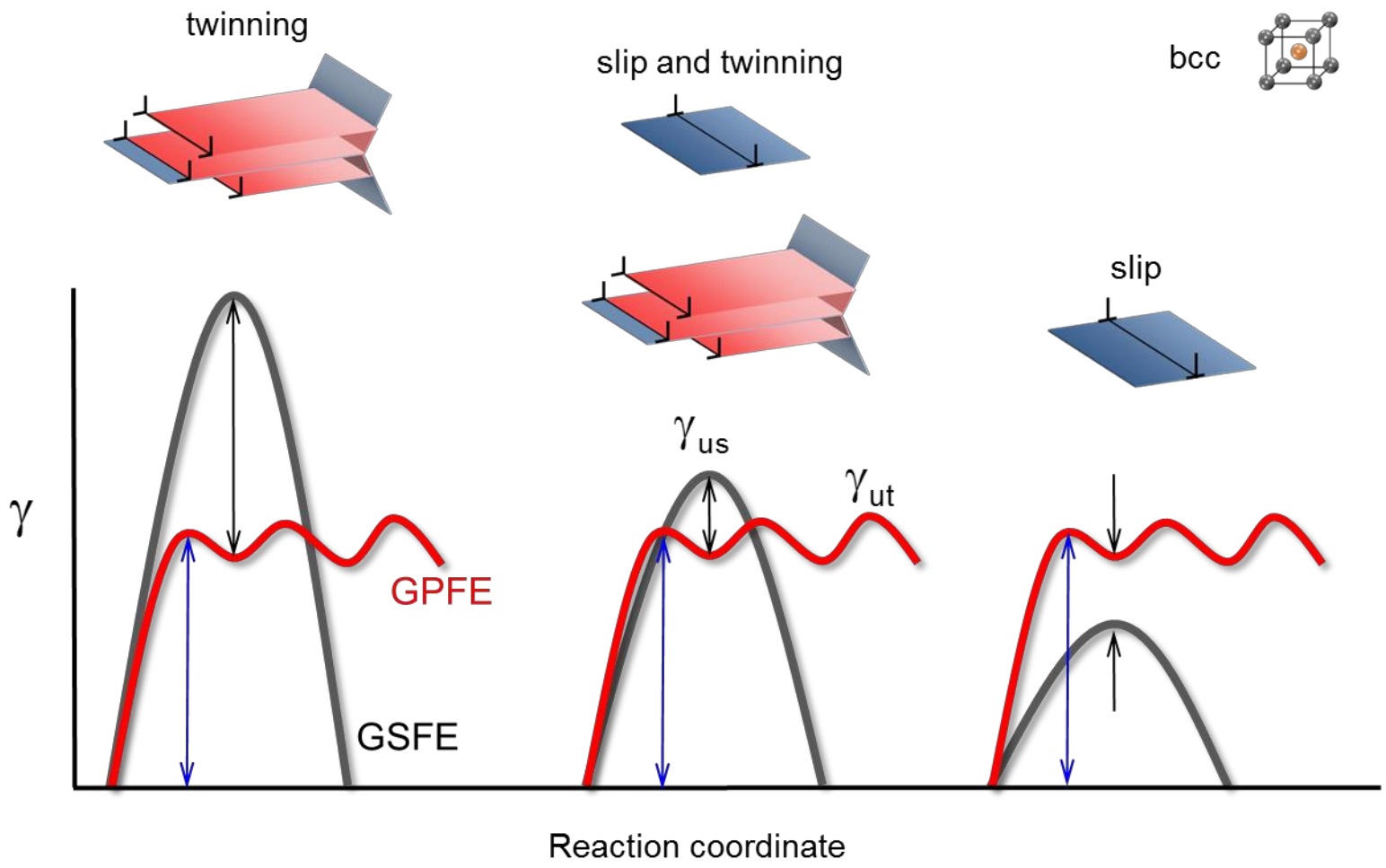
twinning
slip and twinning
bcc
slip
γ
GPFE
GSFE
γus
γut
Reaction coordinate

Figure 11(b)

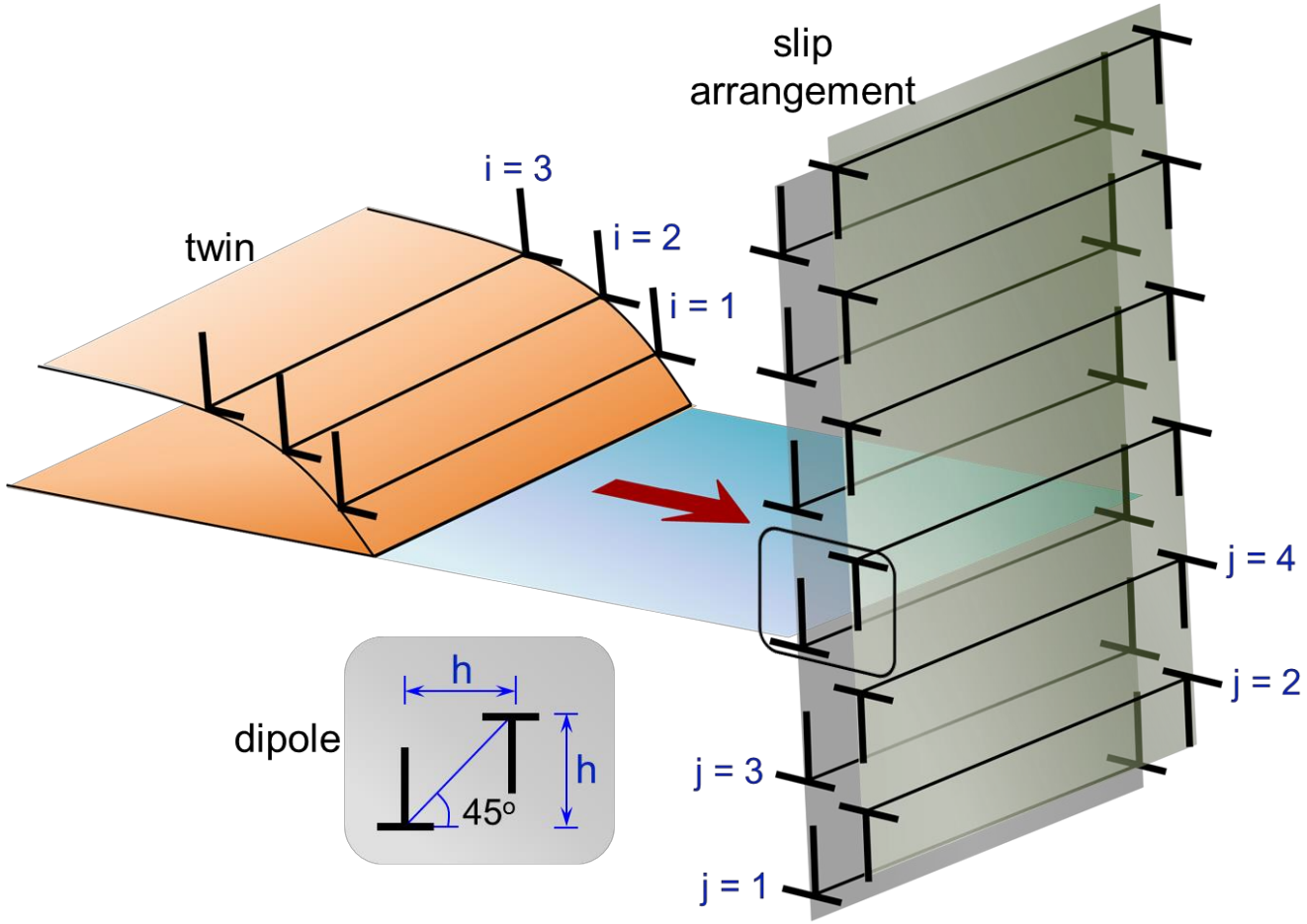

Figure 12

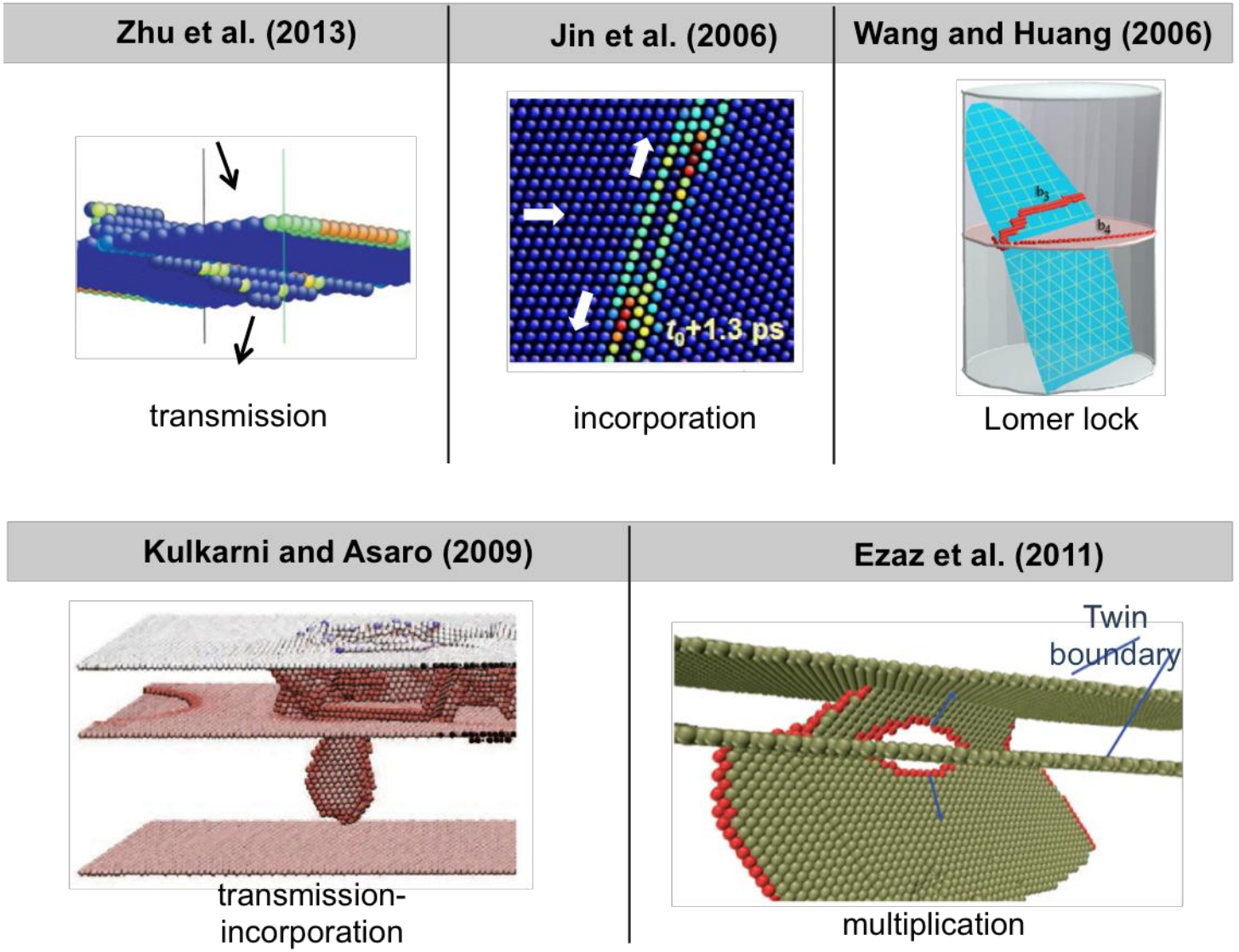
Zhu et al. (2013)
Jin et al. (2006)
Wang and Huang (2006)
t_0+1.3 ps
b_3
b_4
transmission
incorporation
Lomer lock
Kulkarni and Asaro (2009)
Ezaz et al. (2011)
Twin boundary
transmission-incorporation
multiplication

Figure 13

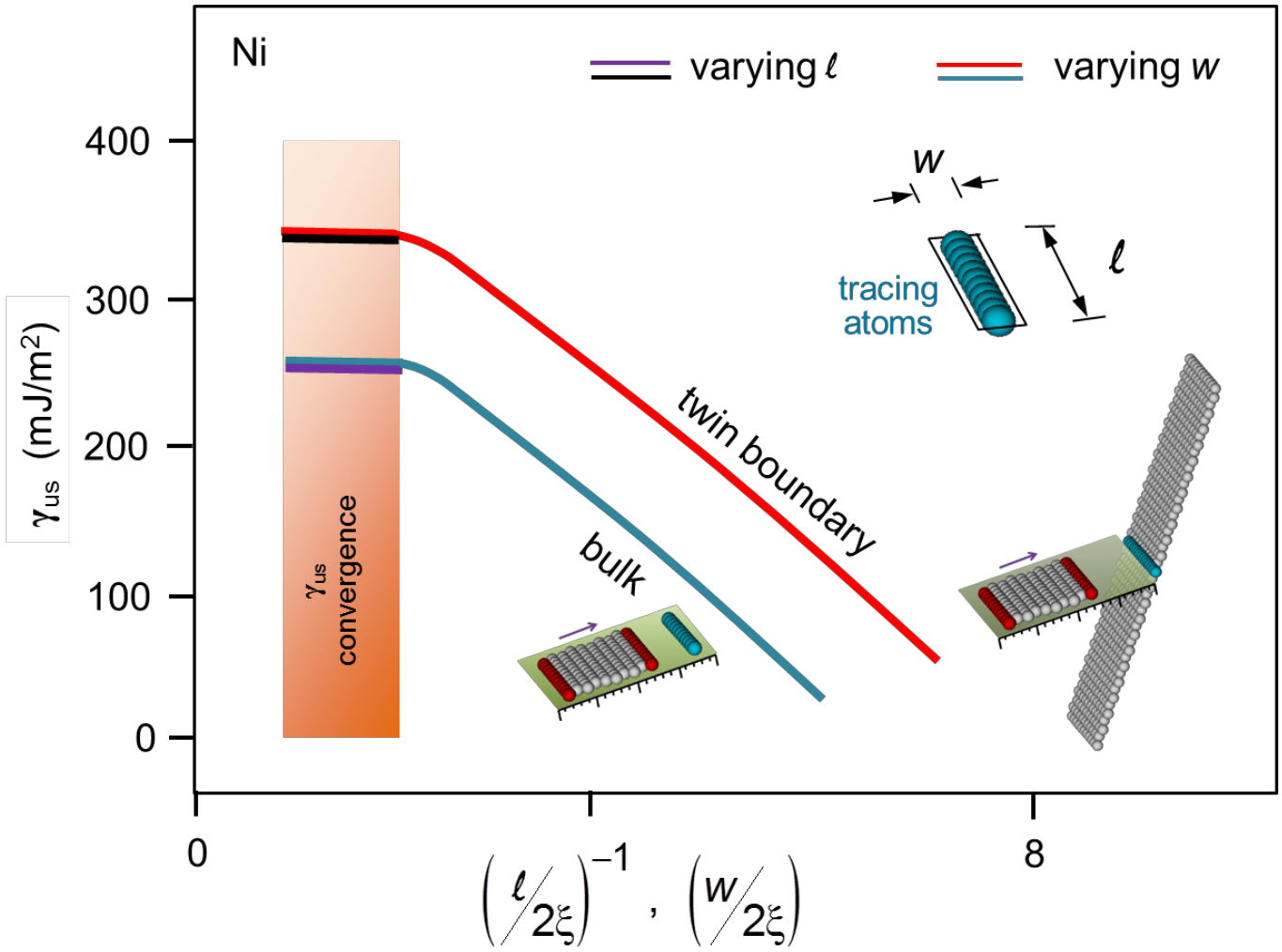
Ni
varying ℓ
varying w
400
300
200
100
0
γ_{us} (mJ/m^2)
γ_{us} convergence
twin boundary
bulk
w
ℓ
tracing atoms
0
8
$\left(\ell/2\xi\right)^{-1}$, $\left(w/2\xi\right)$

Figure 14

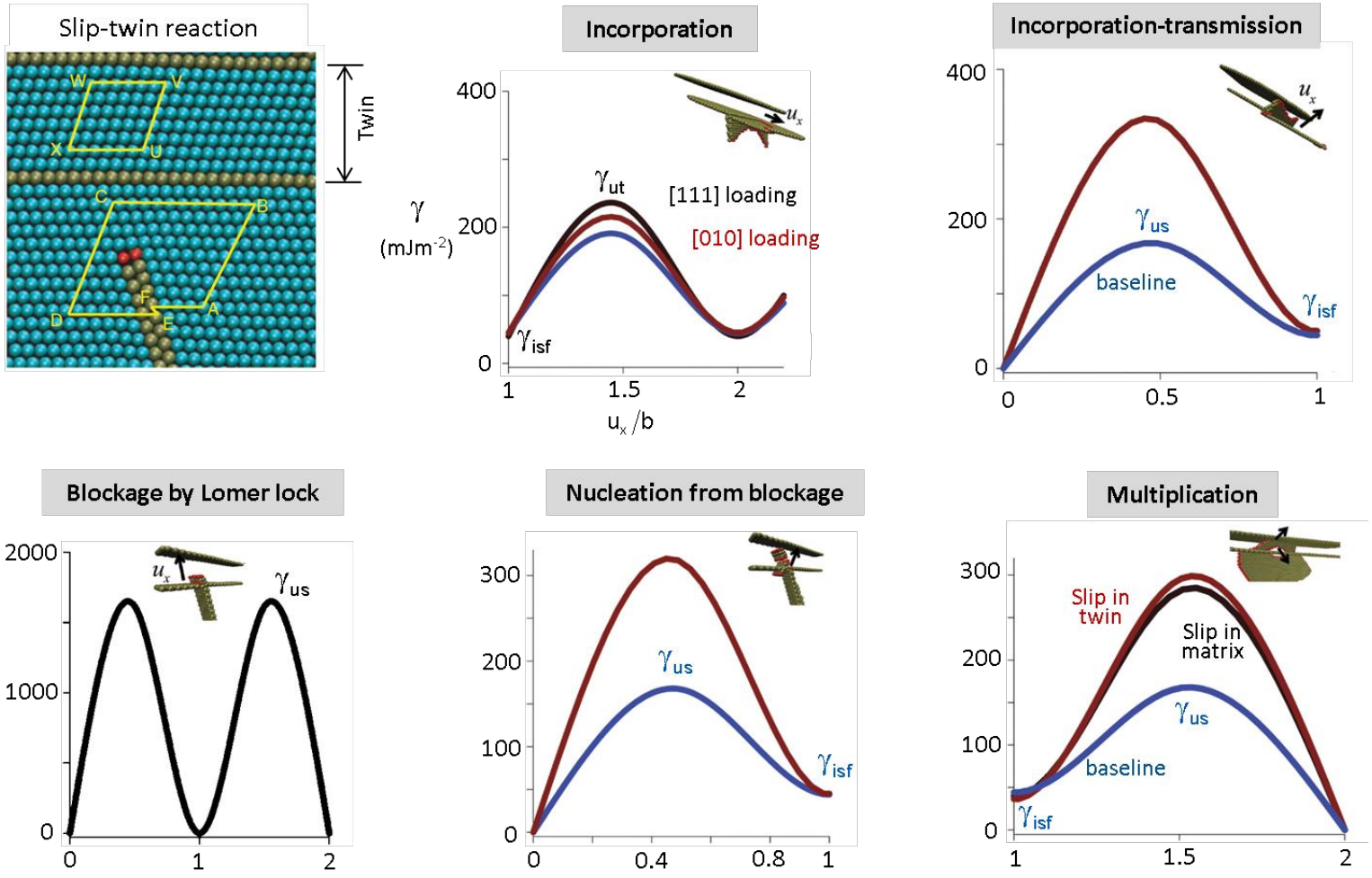
Slip-twin reaction
W
V
X
U
C
B
F
D
E
A
Twin
Incorporation
400
200
0
γ
(mJm-2)
γut
[111] loading
[010] loading
γisf
1
1.5
2
ux /b
ux
Incorporation-transmission
400
200
0
γus
baseline
γisf
0
0.5
1
Blockage by Lomer lock
2000
1000
0
ux
γus
0
1
2
Nucleation from blockage
300
200
100
0
γus
γisf
0
0.4
0.8
1
Multiplication
300
200
100
0
Slip in twin
Slip in matrix
γus
baseline
γisf
1
1.5
2

Figure 15

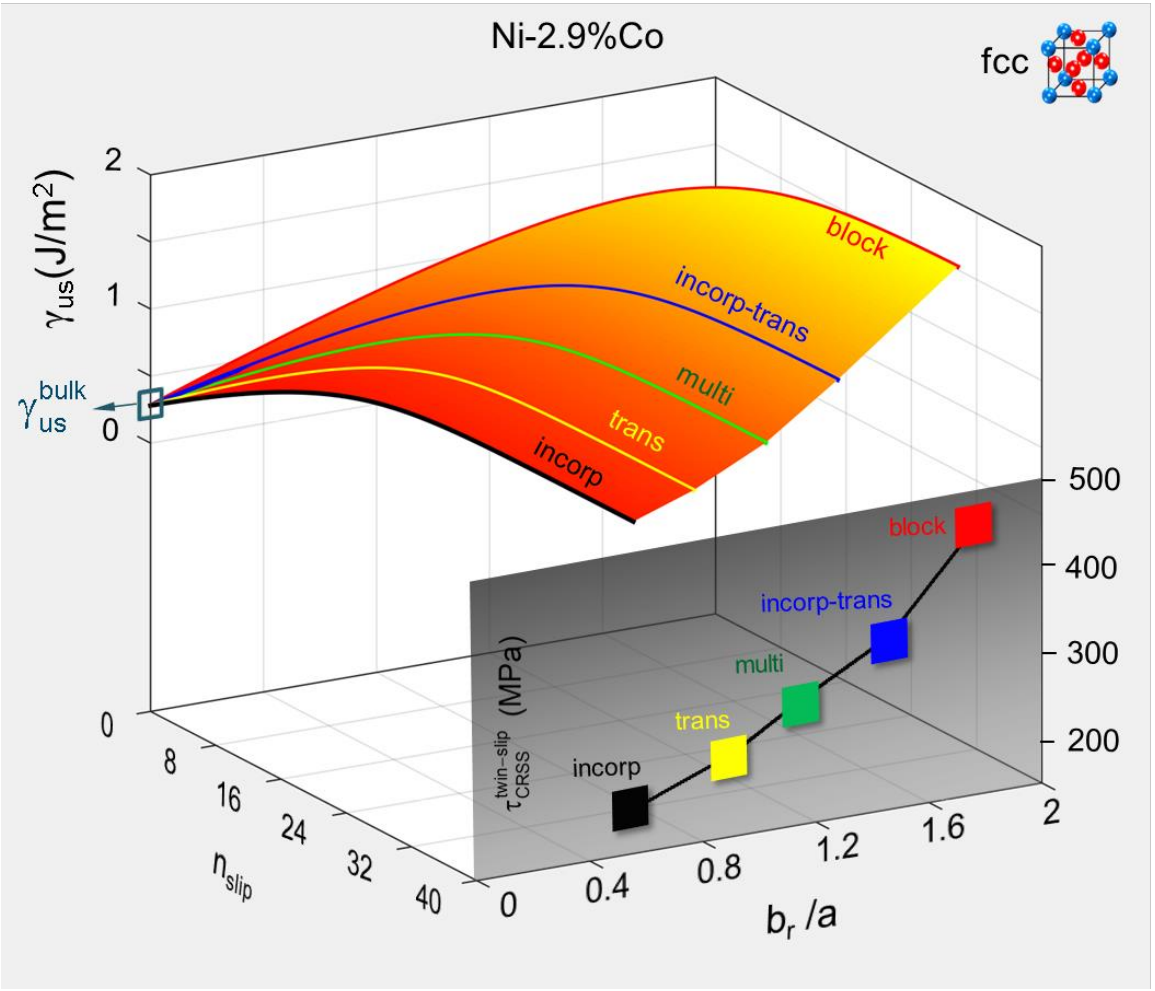
Ni-2.9%Co
fcc
γ_{us}(J/m^2)
2
1
0
γ_{us}^{bulk}
block
incorp-trans
multi
trans
incorp
0
8
16
24
32
40
n_{slip}
500
400
300
200
$\tau_{CRSS}^{twin-slip}$ (MPa)
block
incorp-trans
multi
trans
incorp
0
0.4
0.8
1.2
1.6
2
b_r /a

Figure 16

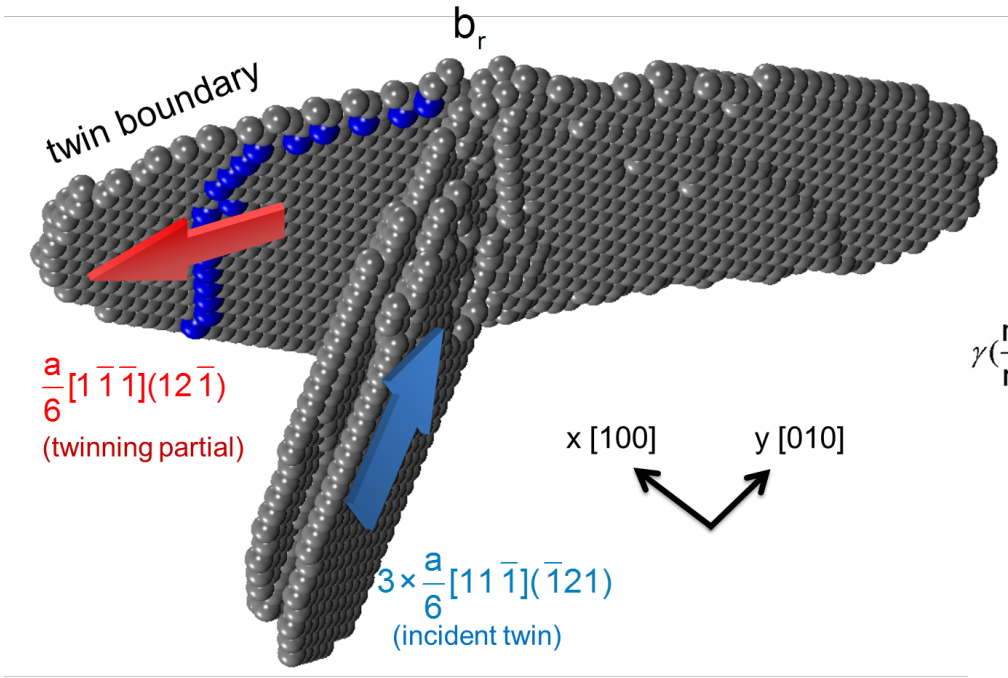

Twin-twin interaction

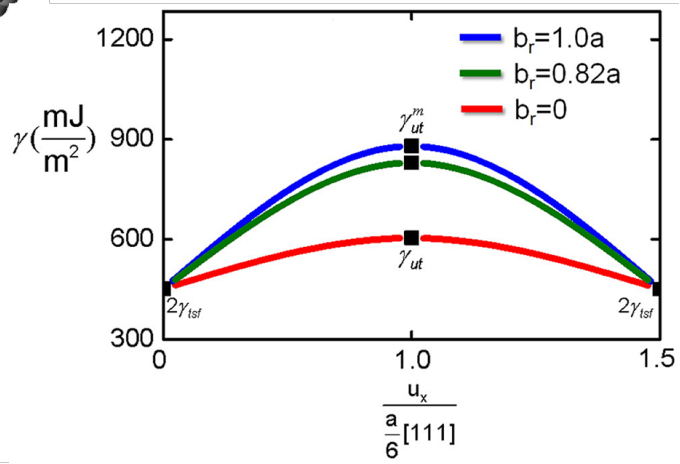

Figure 17

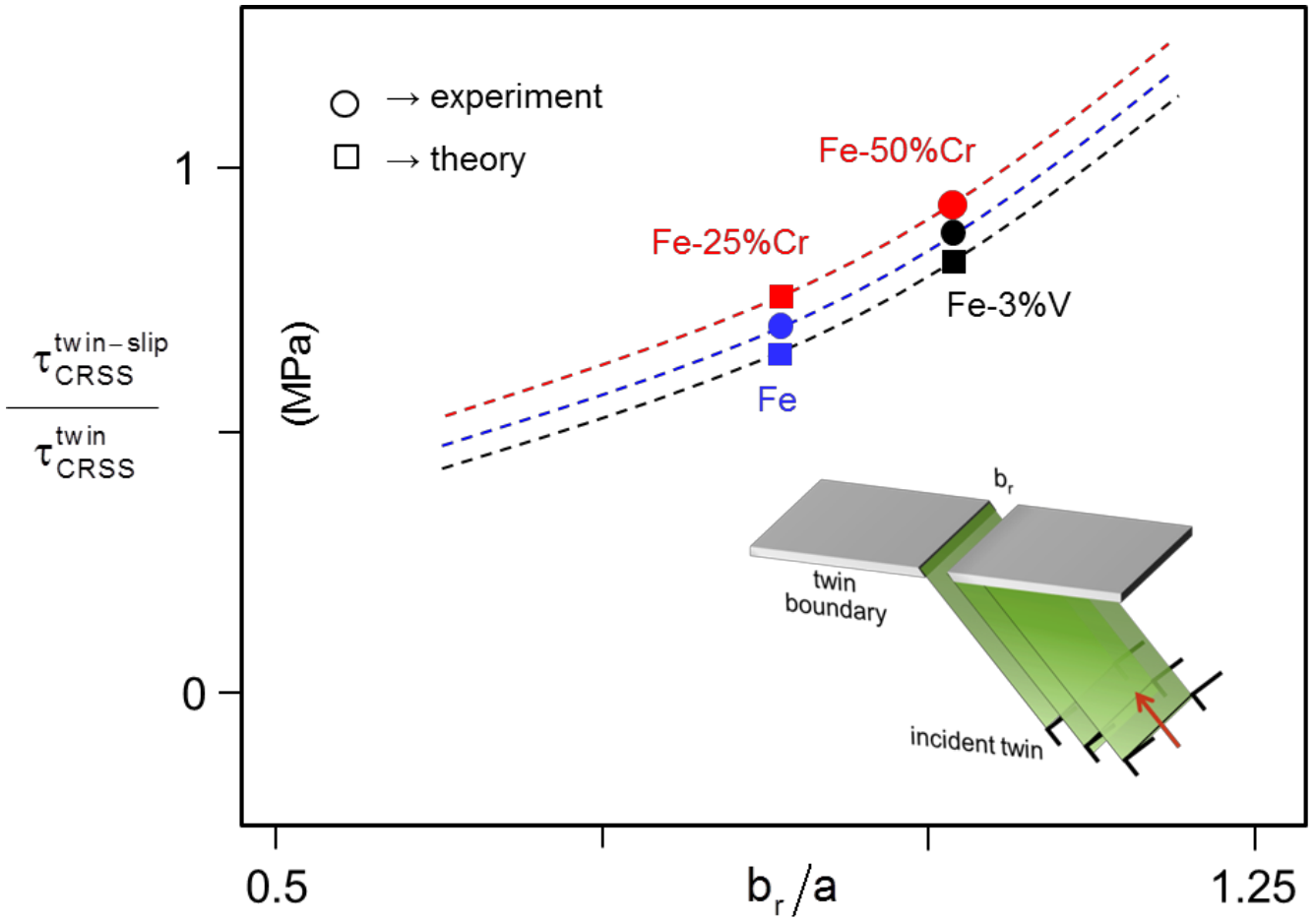
→ experiment
→ theory
Fe-50%Cr
Fe-25%Cr
Fe-3%V
Fe
(MPa)
$\tau_{CRSS}^{twin-slip}$ / τ_{CRSS}^{twin}
1
0
0.5
b_r/a
1.25
b_r
twin boundary
incident twin

Figure 18

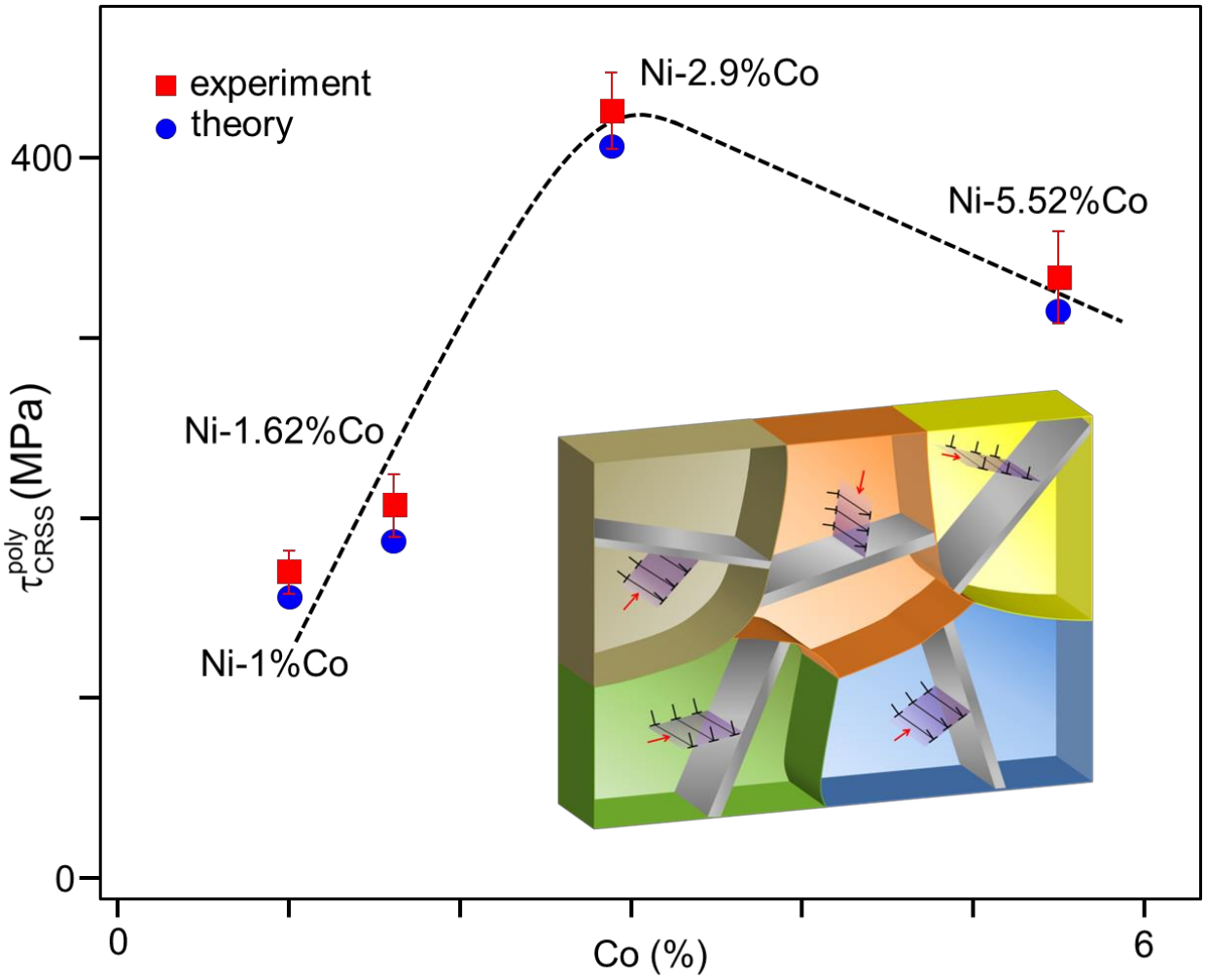
experiment
theory
Ni-2.9%Co
Ni-5.52%Co
Ni-1.62%Co
Ni-1%Co
400
0
τ_{CRSS}^{poly} (MPa)
0
6
Co (%)

Figure 19

Yamakov et al. (2002)	Li et al. (2010)	Shabib and Miller (2009)
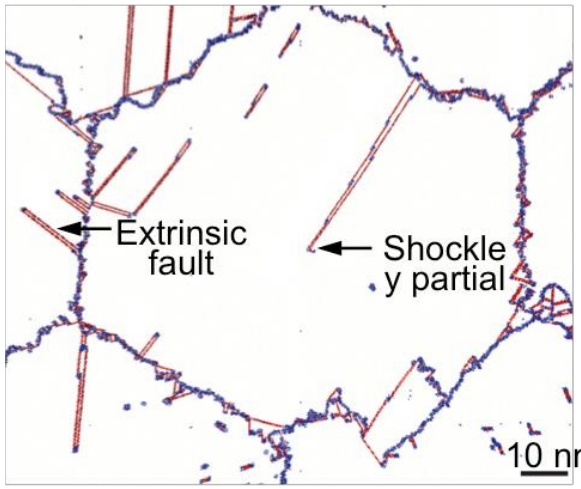	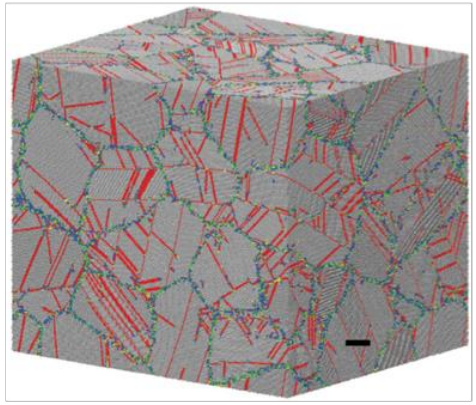	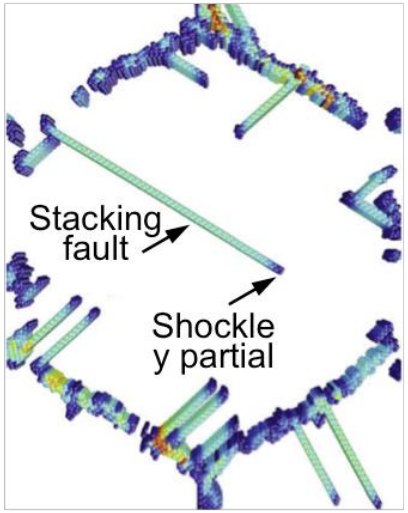
Twin nucleation from grain boundary	Slip intercepting twins in a polycrystal	Slip nucleation from grain boundary

Figure 20

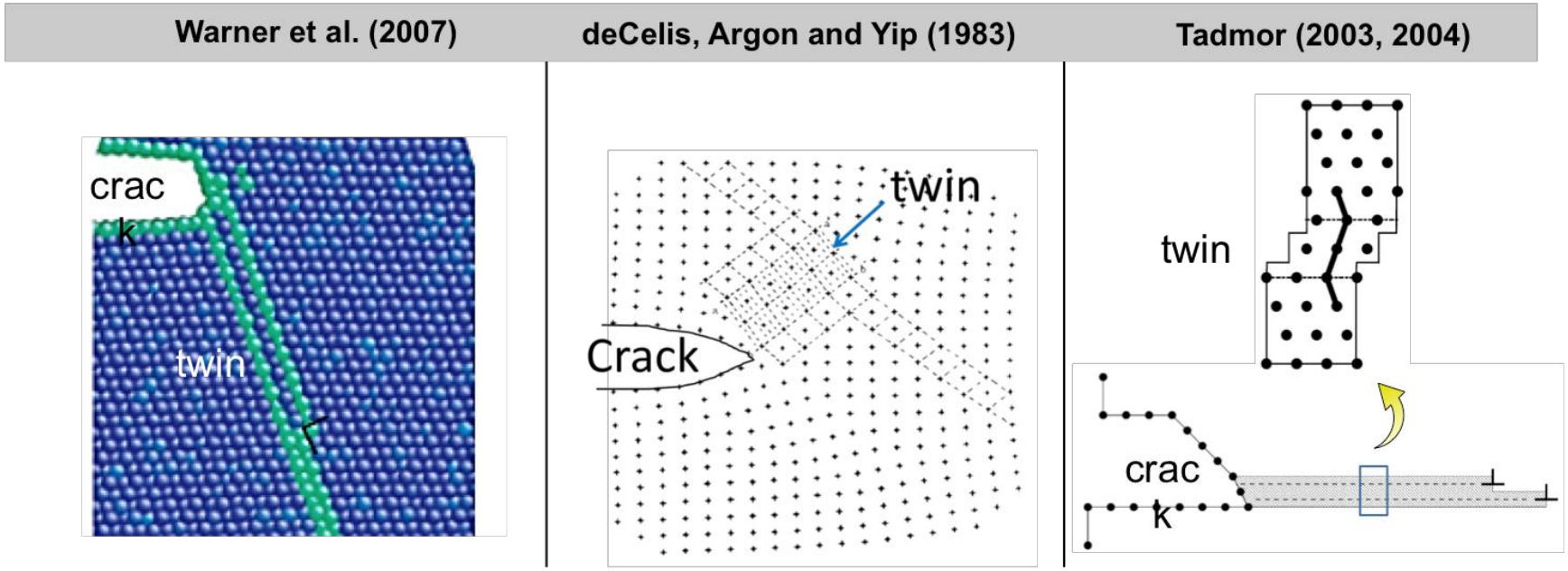
Warner et al. (2007)
deCelis, Argon and Yip (1983)
Tadmor (2003, 2004)
crac
k
twin
twin
Crack
twin
crac
k

Figure 21

Figure captions

Figure 1 – A perspective on the goal of using atomistics to develop physically based theories that can capture the phenomenology of deformation, and thus formulate strategies for property enhancement in novel alloys of wide technological importance.

Figure 2(a) - The Co-Ni crystal under $\langle 111 \rangle$ tension plastically deforms predominantly via twinning and twin-slip slip interactions as confirmed by DIC, EBSD and TEM [52].

Figure 2(b) – Co-Ni compressed along the $\langle 001 \rangle$ orientation demonstrates parallel twinning as the primary deformation mechanism [52].

Figure 2(c) – The deformation of electrodeposited nanocrystalline (as indicated by EBSD analysis) Ni-Co alloys with pre-existent annealing twins shows a strong composition effect [52]. The deformation behavior is found to be characterized by massive slip-twin boundary interactions via electron microscopy.

Figure 3(a) - Fe-Cr single crystal under $[0\bar{1}0]$ tension deforms via interacting deformation twins as evidenced in DIC, EBSD and SEM analyses [34].

Figure 3(b) – The deformation mechanism of Fe-Cr single crystal under [101] begins with slip activities followed by twin nucleation, which causes a stress drop [34]. Subsequently, twin-twin interactions gives rise to hardening as substantiated by DIC, EBSD and TEM techniques.

Figure 3(c) - Polycrystalline Fe-Cr stress-strain response is found to be governed by massive strain transfer across grain boundaries [35] (as confirmed by combined EBSD and DIC studies).

Figure 4 – An illustration of twin nucleation model via pole mechanism in bcc lattice [30, 36]. An expanding slip loop stemming from a sessile dislocation (pole) cross-slips into a perpendicular plane. Subsequently, the dislocation continues to revolve around the pole assisted by further cross-slips and hence generates layers of stacking faults i.e. the twin embryo.

Figure 5 - The dissociation of a screw dislocation with three-fold core in bcc materials into three fraction dislocations under applied stress [40-43]. Two of the fractional dislocations (the most stress ones) cross-glides and becomes parallel to the third one, thereby forming a three-layer twin nucleus.

Figure 6 – Nucleation of a twin embryo through the pole mechanism in fcc lattice is proposed to be controlled by a simultaneous process of mobile jog formation and dislocation loop expansion [44-46]. Expanding slip loops from two adjoining planes eventually interconnect to form a continuous spiral, ultimately leading to the twin nucleation.

Figure 7 – Full dislocations dissociate into partials connected by intrinsic stacking faults [47]. Two extended dislocations from adjoining planes form a two-layer fault i.e. an extrinsic stacking fault. Interaction between two extrinsic stacking faults leads ultimately to twin formation.

Figure 8 – The atomistic configuration of a deformation twin produced from lattice shearing induced by consecutive glide of slip [52].

Figure 9 – To generate a γ surface, crystal blocks consisting of atoms are rigidly sheared in atomic simulations. The atomic structures of the perfect lattice and the one corresponding to an intrinsic stacking fault are shown [52] as computed from DFT simulations.

Figure 10(a) – Generalized stacking fault energy (GSFE) for Co-Ni alloys which represents the energy pathway for the nucleation of an extended dislocation [52] connected by an intrinsic stacking fault.

Figure 10(b) - Generalized planar fault energy (GPFE) for Co-Ni alloys[52] as an example. The GPFE represents the twinning energy pathway encompassing the formation of a single-layer intrinsic stacking fault first, then a two-layer extrinsic stacking fault and finally a three-layer twin nucleus. Further shearing on consecutive planes results in the twin growth (migration) process.

Figure 10(c) – Comparison among the GSFE and GPFE in bcc Fe and Fe-Cr alloys. There are two distinct types of twin boundaries in bcc alloys, namely, isosceles and reflective ones [71] which are favored differently from one material (e.g. Fe) to another (e.g. Fe-Cr).

Figure 11(a) – Relative sizes of the fault energetics (GSFE and GPFE) and their implication regarding the preference for a certain defect nucleation for fcc lattice [3, 58-60].

Figure 11(b) - Possible shapes of fault energy surfaces and the likely defect mechanism scenario in bcc lattice.

Figure 12 - Modeling of twin-slip interaction based on dislocation mechanics whereby a propagating three-layer twin approaches a dislocation dipole arrangement [52]. The atomistic contributions are considered in the form of GPFE representing the discrete lattice during the process.

Figure 13 – Five different types of slip-twin boundary interaction mechanisms studied in molecular dynamics simulations: transmission [23], incorporation [27] (shown after 1.3 picoseconds from the beginning, t_o) Lomer lock formation [25], transmission-incorporation [98] and multiplication [94].

Figure 14 – The “tracing atom” method for computing the extrinsic magnitude of γ_{us} from molecular dynamics simulations [104]. The convergence criteria of the energy parameter is obtained at high ℓ and low w, which are the length and width of the tracing area respectively.

Figure 15 – Fault energy profile for various slip-coherent twin boundary interaction mechanism in fcc Cu [94]. Incorporation process has the lowest energy barrier while the blockage case the highest. The blue curves designated “baseline” represents the GSFE profile for bulk lattice shearing (i.e. absence of residual slip b_r). The reason the GSFE curves specific to the reactions are elevated is that b_r creates local stress, which makes glide difficult for subsequent incidence.

Figure 16 – Evolution of energy barriers for various slip-twin interaction mechanisms with respect to the number of incident slip (n_{slip}) and the predicted frictional stresses ($\tau_{CRSS}^{twin-slip}$) [105].

Figure 17 – An approaching twin consisting of three $\frac{a}{6}[11\bar{1}]$ type twinning partials intercept a pre-existent twin boundary [71] in bcc Fe-Cr alloy. The resultant reaction is the incorporation of the twinning partials on the boundary leaving a residual dislocaiton (br) behind at the interception site. Depending on the magnitude of br (which can be obtained by modulating the Schmid factor or changing single crystal loading direction), the GSFE profile will be altered as shown on the right.

Figure 18 – Comparison between the predicted twin-twin interaction stress ($\tau_{CRSS}^{twin-twin}$) and the experimental one in several bcc alloys [71].

Figure 19 – Comparison between the predicted and experimental critical resolved shear stresses in polycrystalline NiCo alloys (in the presence of annealing twins) [52].

Figure 20 – Molecular dynamics simulation of polycrystalline deformation behaviors. From left to right: Nucleation of twins from grain boundaries in nanocrystalline Al [115]; a nanocrystalline Cu structure with annealing twins, which upon deformation results in massive slip-interface interactions [117]; Shockley partials emerging from grain boundaries in Cu [116].

Figure 21 – Study of cracktip twinning behavior using atomistics concept. Competition between twin and slip nucleation from a crack is correlated with the relative size/shape of GSFE/GPFE curves [59, 60, 69, 123].

Table 1 – A summary of literature data on the g_{isf}, γ_{us} and g_{ut} for various fcc metals for comparison [61].

Materials	g_{isf} (mJm^{-2})	γ_{us} (mJm^{-2})	g_{ut} (mJm^{-2})
Pb	49	87	92
Ag	18	133	143
Au	33	134	148
Cu	41	180	200
Ni	110	273	324
Pd	168	287	361
Pt	324	339	486
Al	130	162	215

Table 2(a) – Comparison of theoretical and experimental twin nucleation stresses in bcc materials [71] (see text for equation details).

The Burgers vector ($\vec{b}$) for twinning partial is $\frac{a}{6}\langle 111\rangle$ (i.e. b = $\frac{a\sqrt{3}}{6}$), where a is the alloy-specific lattice constant.

Mechanism	Materials	Major input parameters for prediction	Predicted τ_{CRSS}^{twin} (MPa)	Experimental τ_{CRSS}^{twin} (MPa)
twin 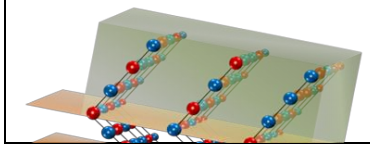	Fe-3%V	a = 0.2866 nm γ_{us} = 615 mJm^{-2} γ_{ut} = 596 mJm^{-2}	109	90

	Fe	a = 0.2851 nm γ_{us} = 617 mJm^{-2} γ_{ut} = 628 mJm^{-2}	190	170
	Fe-50%Cr	a = 0.2851 nm γ_{us} = 1060 mJm^{-2} γ_{ut} = 752 mJm^{-2}	218	203 ± 13
	Fe-25%Ni	a = 0.2882 nm γ_{us} = 525 mJm^{-2} γ_{ut} = 549 mJm^{-2}	377	398

Table 2(b) – Comparison between the theoretical and the experimental CRSS levels for slip nucleation, twin nucleation and twin-slip interaction in fcc Co-33%Ni alloy [52].

Mechanism	Equations	Input parameters	Theoretical τ_{CRSS} (MPa)	Experimental τ_{CRSS} (MPa)
Slip nucleation	$\tau_{CRSS}^{slip} = \frac{1}{b}\frac{\partial E_{GSFE}(\gamma_{isf},\gamma_{us})}{\partial u}\Big\vert_{max}$	$\gamma_{us} = 205\ mJ/m^2$ $\gamma_{isf} = 20\ mJ/m^2$ $b = a_{Co-Ni}/\sqrt{6}$ $a_{Co-Ni} = 3.521\ \mathring{A}$	14	15

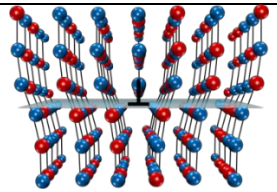				
Twin nucleation 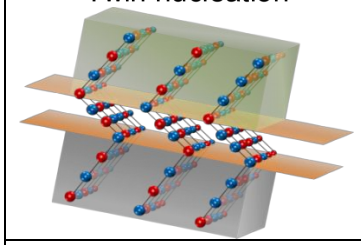	$\tau_{CRSS}^{twin} = \frac{E_{interaction} + E_{GPFE-nucleation}(\gamma_{tsf}, \gamma_{ut})}{tw\varepsilon_{twin}}$	$\gamma_{ut} = 216\ mJ/m^2$ $\gamma_{tsf} = 10\ mJ/m^2$ $t = 3a_{Co-Ni}/\sqrt{3}$ $w \approx 10t$ $\varepsilon_{twin} = 1/\sqrt{2}$	26	27
Onset of twin-slip interaction 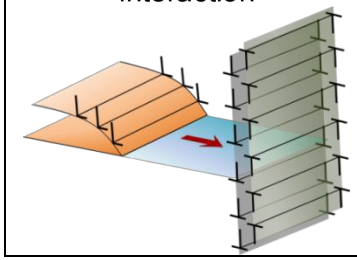	$\tau_{CRSS}^{twin-slip} = \frac{E_{twin\text{-}wall\ interaction} + E_{GPFE-migration}(\gamma_{tsf}, \gamma_{ut})}{td\varepsilon_{twin}}$	$\gamma_{ut} = 216\ mJ/m^2$ $\gamma_{tsf} = 10\ mJ/m^2$ $d \approx 3\ nm$ $\varepsilon_{twin} = 1/\sqrt{2}$	38	39

Table 3 – The molecular dynamics approach of computing the $\tau_{CRSS}^{twin-slip}$ in Ni-Co alloys [52].

Twin boundary-slip interaction mechanisms		Dislocaiton type	b_r/a (saturated after multiple incidence)	$\tau_{CRSS}^{twin-slip}$ (MPa)
Incorporation	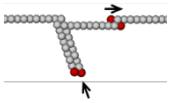	Screw	0.55	175
Transmission	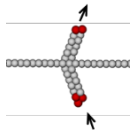	Edge	0.76	230
Multiplication	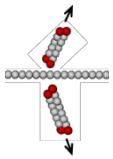	Mixed	1.02	280
Transmission-incorporation	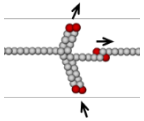	Mixed	1.27	336
Blockage by Lomer lock	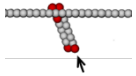	Mixed	1.70	445

Table 4 – Summary of theories reviewed in this paper contributing to twining energetics and critical stress prediction in fcc and bcc materials.

	Investigators	Model description	Model impact
Continuum	Meyers et al. [67]	Formulating deformation kinetics of twinning	- lays foundation for continuum-based analysis of temperature and strain-rate effects of deformation twinning
	Kalidindi et al., Staroselsky	Thermodynamic analysis of deformation twinning	- establishes a work-energy

	et al., Fischer et al. [62, 63, 68]		balance for twin embryo formation based on continuum dislocation mechanics
	Miura et al., Karaman et al. [50, 66]	Rationalization of twining propensity originating from alloying	- utilize γ_{isf} to predict critical stress for twin nucleation
Mesoscale	Sleeswyk et al., Ogawa et al., Priestner and Leslie, Lagerlof [40-43, 46]	Mechanism of Twin embryo nucleation in bcc materials	- provides a mechanistic interpretation of twin nucleation considering dissociation of a three-fold slip core
	Cottrell and Bilby [36]	Mechanism of twin nucleus formation in bcc lattice	- explains twin nucleation with the aid of a slip acting as a source (pole) of stacking fault emission
	Venables [44, 45, 64]	Nucleation of twin embryo in fcc lattice via double-pole mechanism	- Proposes a double pole to account for the relative ease of layer-by-layer stacking fault piling leading to twin embryo
	Remy [7, 8, 19]	Geometry of twinning dislocations intercepting another twin	- provides detailed analysis of Burgers vector conservation in twin-twin interactions in post-yield behavior
	Mahajan and Chin [47]	Mechanism of twin nucleus formation in fcc lattice	- explains fcc twinning mechanism which occurs via interaction between two extrinsic stacking faults
Atomistics	Ogata et al., Swygenhoven et al., Siegel et al., Cai et al. [3, 4, 56-58]	Prediction of twinning γ energies (i.e. GPFE)	- demonstrates feasibility of utilizing modern atomistic simulations tools to compute twinning energy barriers (by rigid shear of crystal half-spaces)

	Yamakov et al. Asaro and Suresh, Jin et al., Zhu et al., Deng and Sansoz, Kulkarni et al. Shabib et al., Li et al., Ezaz et al. [5, 23, 27, 86, 87, 94, 98, 115-117]	Annealing twins (with coherent twin boundaries) influencing deformation mechanism at nanoscale	- investigates roles of pre-existent annealing twins on mechanical response - explores slip-coherent twin boundary interactions, their energetics, and eventual role of controlling strength and ductility
	deCelis et al., Tadmor et al., Warner et al. [59, 60, 123]	Atomistics of twining as relates to cracktip plasticity	- introduces a detailed model using energy barriers (γ_{us} , γ_{ut}) in addressing fracture problem in fcc materials
	Kibey et al., Chowdhury et al., Ojha et al. [39, 52, 71, 76]	- Atomistics of twinning and twin-slip interaction and prediction of critical stress	- predicts GPFE profiles for twinning in pristine lattice and also subjected to residual slip accumulation - predicts critical stresses for intrinsic or extrinsic twinning mechanisms